

Mathematics and Pattern Formation in Chemistry and Biology

Peter Schuster

Institut für Theoretische Chemie, Universität Wien, Austria

and

The Santa Fe Institute, Santa Fe, New Mexico, USA



Tagung über Schulmathematik

TU Wien, 28.02.2006

Web-Page for further information:

<http://www.tbi.univie.ac.at/~pks>

1. Equilibrium structures and dissipative patterns
2. Spatio-temporal patterns in chemical reactions
3. Patterns in development
4. Genetic and metabolic networks
5. Patterns in neurobiology

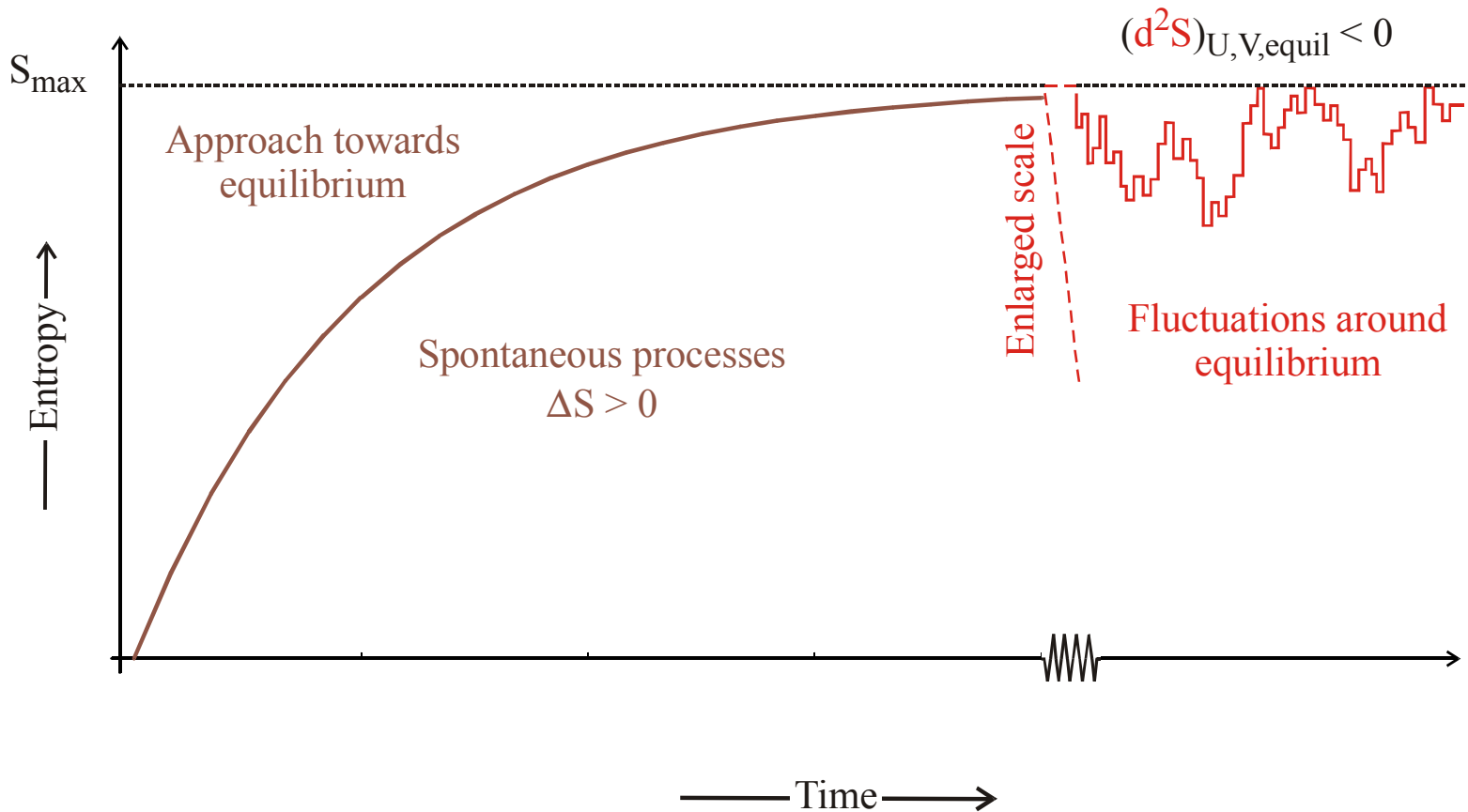
1. **Equilibrium structures and dissipative patterns**
2. Spatio-temporal patterns in chemical reactions
3. Patterns in development
4. Genetic and metabolic networks
5. Patterns in neurobiology

Equilibrium thermodynamics is based on two major statements:

1. *The energy of the universe is a constant (first law).*
2. *The entropy of the universe never decreases (second law).*

Carnot, Mayer, Joule, Helmholtz, Clausius,

D.Jou, J.Casas-Vázquez, G.Lebon, *Extended Irreversible Thermodynamics*, 1996



Entropy and fluctuations at equilibrium

Environment

$$dS_{\text{env}} > 0$$

Selforganization

$$dS = dS_i + dS_e < 0$$

$$dS_i > 0$$

$$\leftrightarrow$$

$$dS_e < 0$$

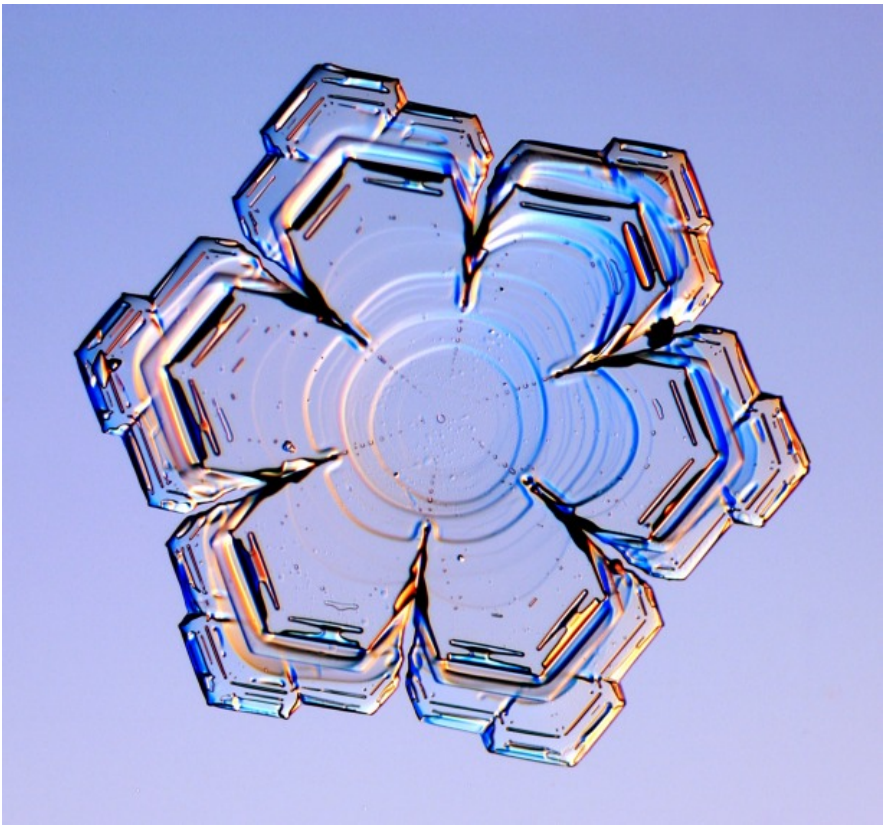
$$dS_{\text{tot}} = dS + dS_{\text{env}} > 0$$

Entropy is equivalent to disorder. Hence there is no spontaneous creation of order at equilibrium.

Self-organization is spontaneous creation of order.

Self-organization requires export of entropy to an environment which is almost always tantamount to an energy flux or transport of matter in an open system.

Entropy production and self-organization in open systems

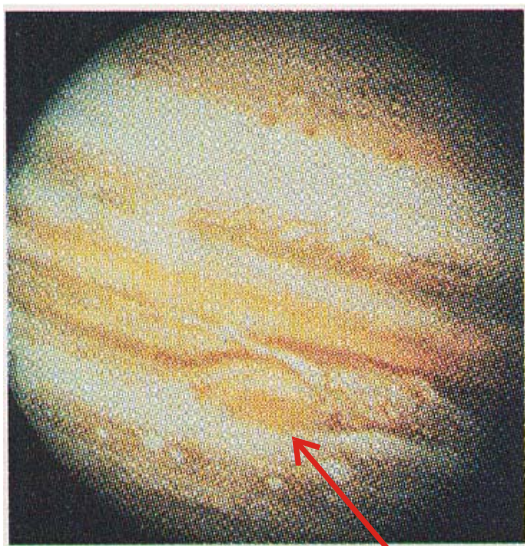


Snowflakes as examples of equilibrium structures that do not require energy for their maintenance

Five examples of self-organization and spontaneous creation of order

- *Hydrodynamic pattern formation in the atmosphere of Jupiter*
- *Pattern formation in heated fluids*
- *Pattern formation in chemical reactions*
- *Morphogenesis in the development of embryos*
- *Patterns in neurobiology*

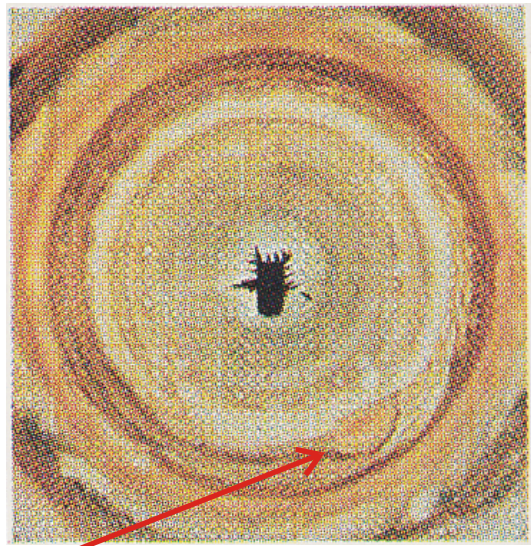
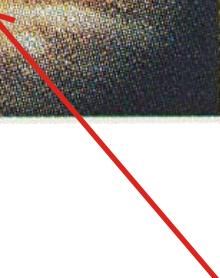
Examples of self-organization and pattern formation



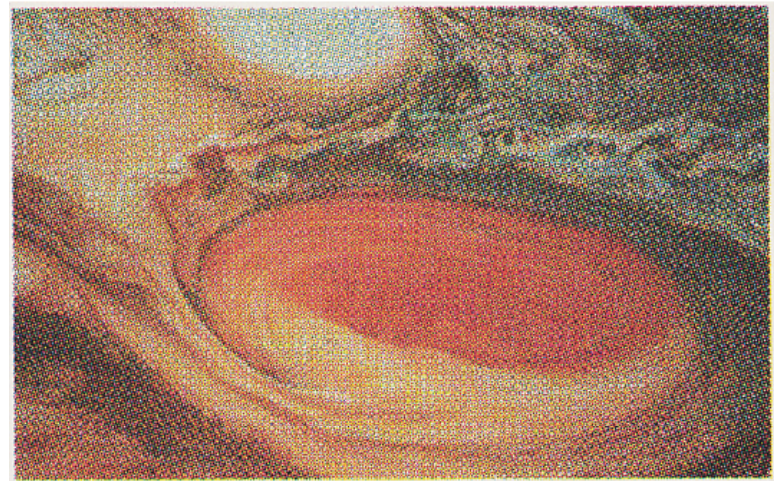
South pole



Red spot



View from south pole



Jupiter: Observation of the gigantic vortex

Picture taken from James Gleick, *Chaos*. Penguin Books, New York, 1988

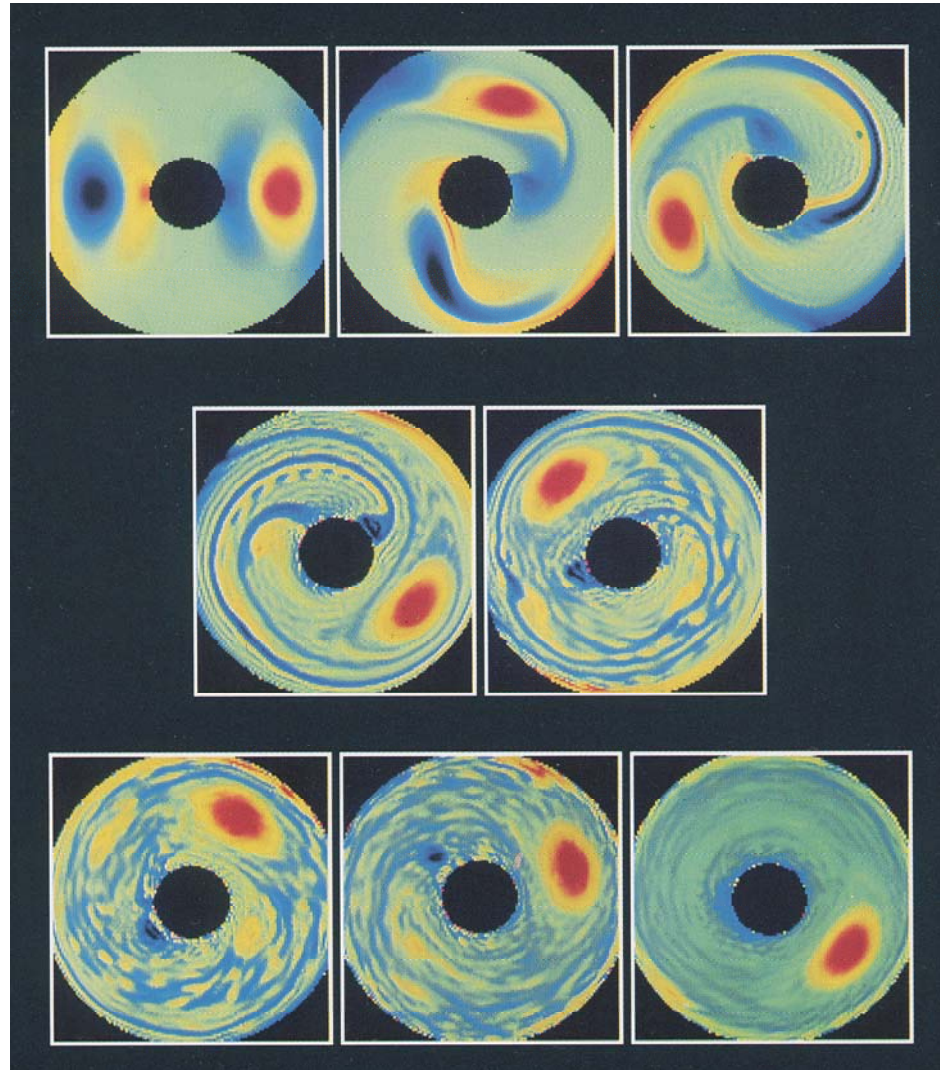
Computer simulation of the gigantic vortex on Jupiter

View from south pole

Particles turning
counterclockwise



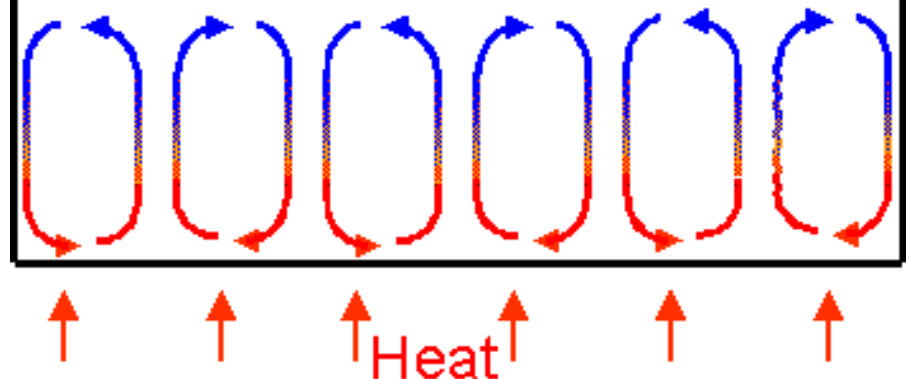
Particles turning
clockwise



Jupiter: Computer simulation of the giant vortex

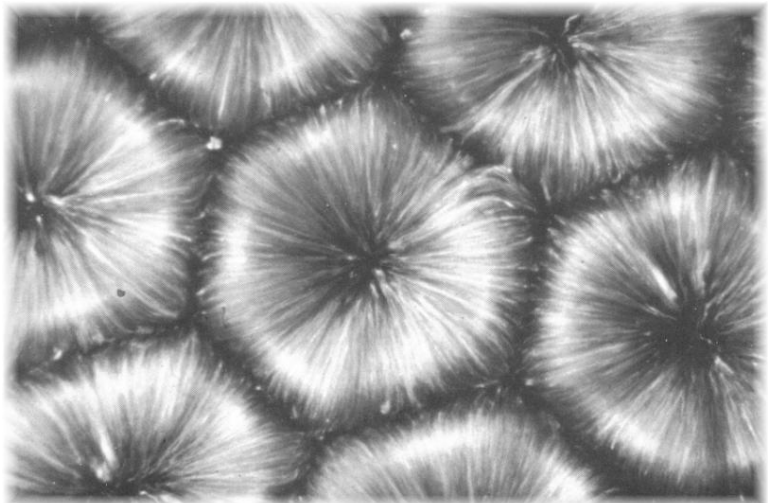
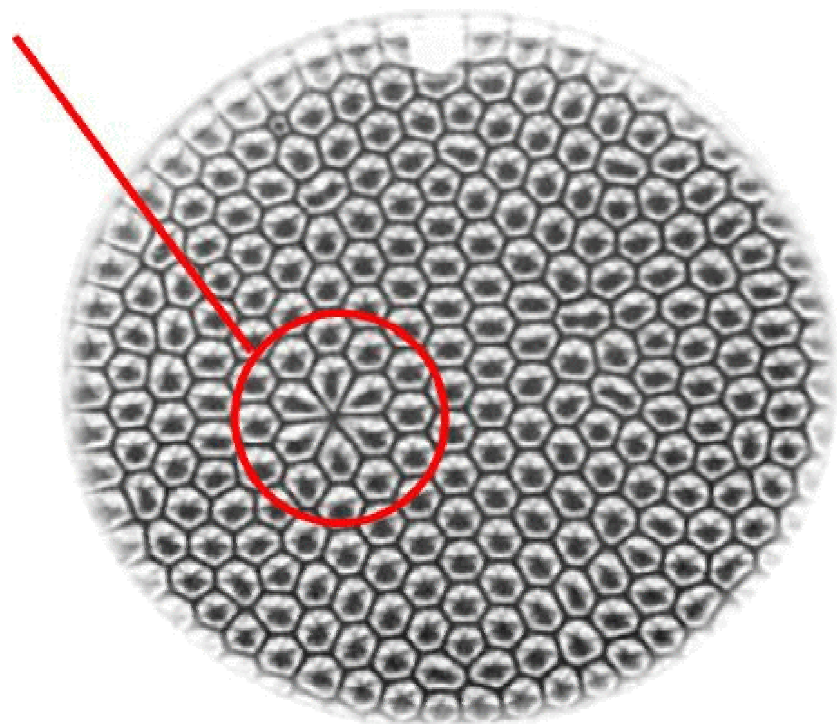
Philip Marcus, 1980. Picture taken from James Gleick, *Chaos*. Penguin Books, New York, 1988

Fluid cools by losing heat from surface

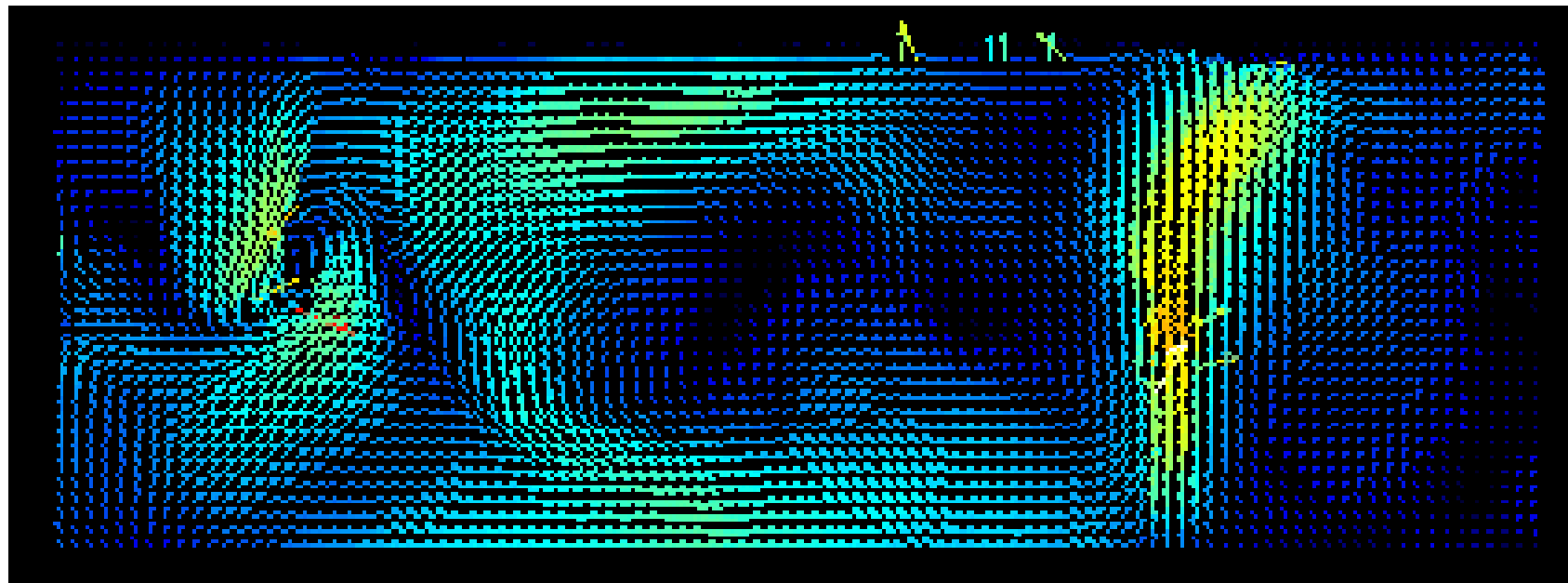


Convection cell

Warm, low density fluid rises
Cool, high density fluid sinks



Rayleigh-Benard convention cells in heated fluids

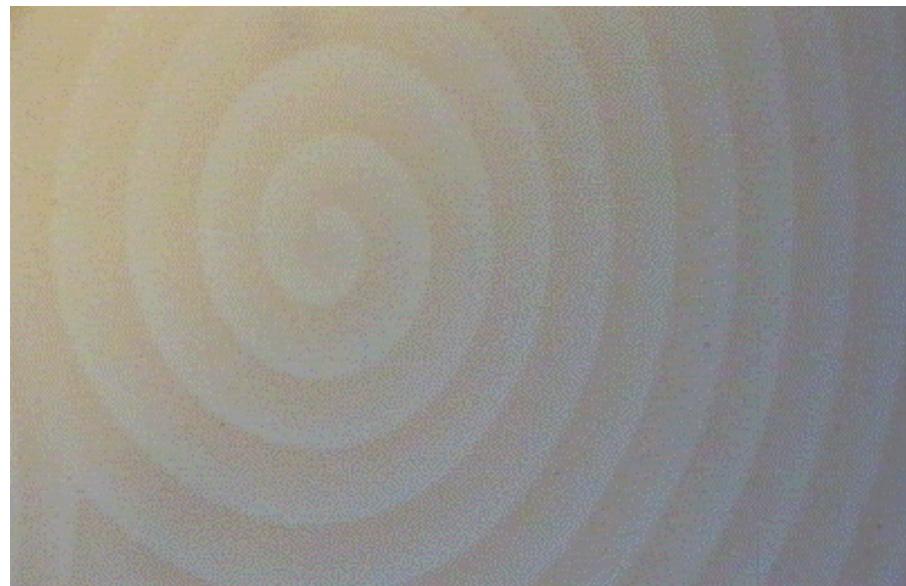


Alberto Petracci. Particle image velocimetry (PIV) measurement of convective flow in a Raleigh-Benard convection cell of dimension $60 \times 60 \times 20$ mm

CHEMICAL ROTORS



Spatio-temporal pattern in the
Belousov-Zhabotinskii reaction



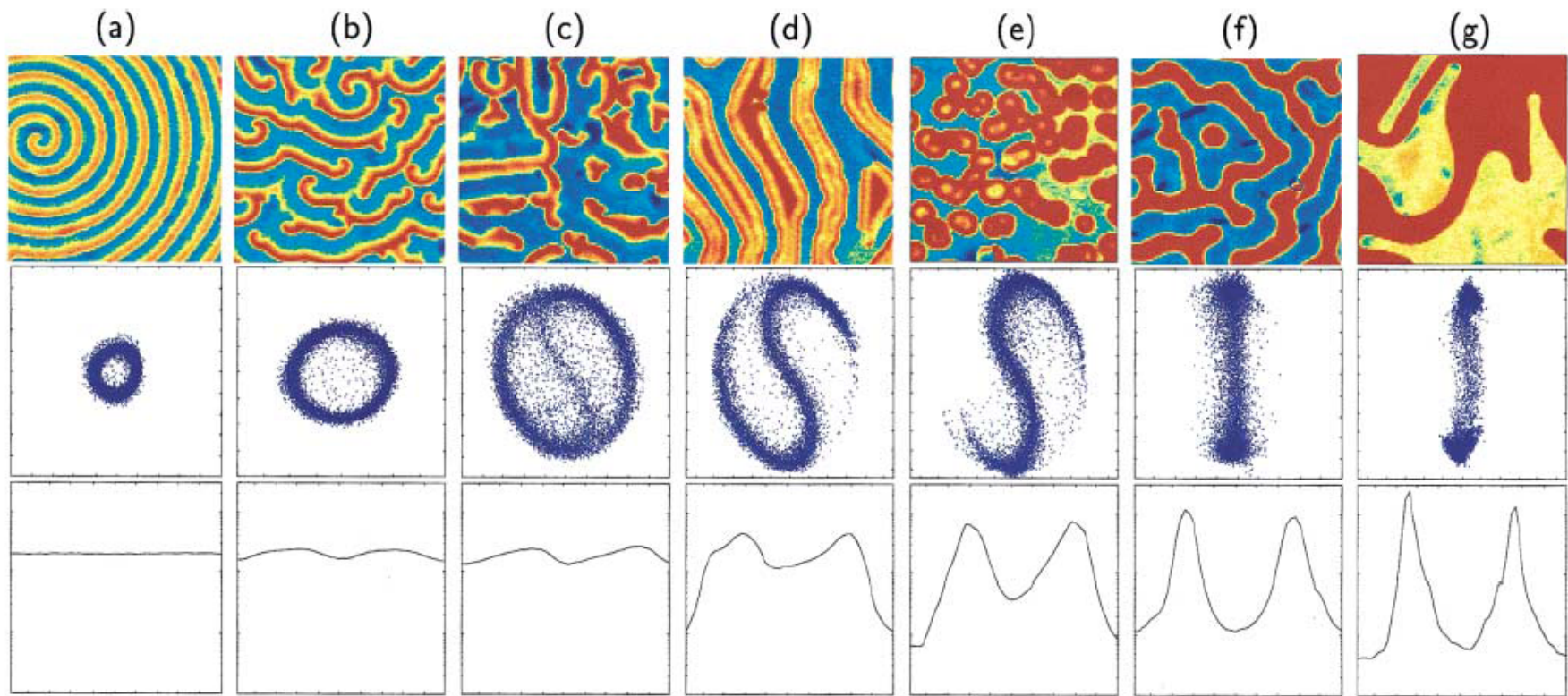
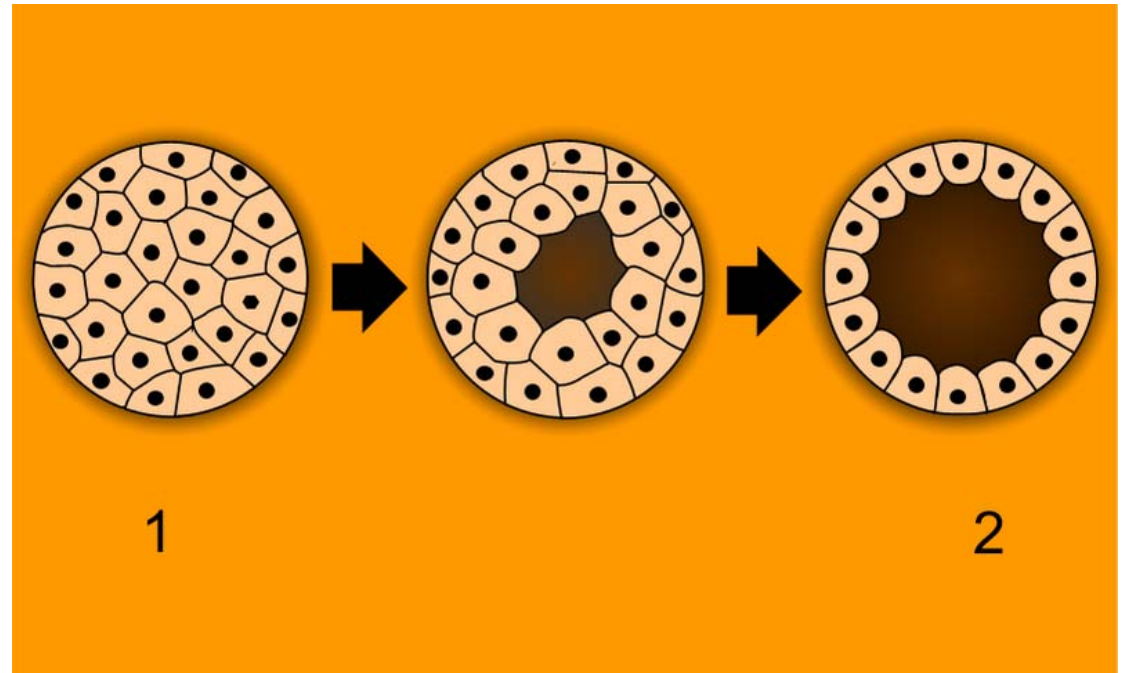


FIG. 2 (color). (top row) Reactor images ($9 \times 9 \text{ mm}^2$) of different observed patterns, presented using a rainbow (false) color map: (a) unforced rotating spiral wave, (b) rotating spiral wave, (c) mixed rotating spiral and standing wave pattern, (d)–(g) qualitatively different standing wave patterns. Patterns (b)–(g) exhibit a 2:1 resonance in the temporal power spectrum of the pattern. (middle row) The complex Fourier amplitude a for each image: the abscissa is $\text{Re}(a)$; the ordinate is $\text{Im}(a)$. Each point in the complex plane corresponds to the temporal Fourier amplitude a of a pixel in the image after frequency demodulation at $f/2$. (bottom row) Histograms of phase angles of all the pixels in each image; the abscissa range is $[0, 2\pi]$ radians and the ordinate range is arbitrary. Chemical conditions are given in [9]. For each pattern the parameter values of $f(\text{Hz})$ and $\gamma^2(\text{W/m}^2)$ are, respectively, (a) 0, 0; (b) 0.1000, 119; (c) 0.0625, 214; (d) 0.0556, 248; (e) 0.0417, 358; (f) 0.0455, 386; (g) 0.0385, 412, and correspond to the circled points in Fig. 1.

Pattern formation in the Belousov-Zhabotinskii reaction

Anna L. Lin, Matthias Bertram, Karl Martinez, and Harry L. Swinney, *Phys.Rev.Letters* **84**, 4240 (2000)

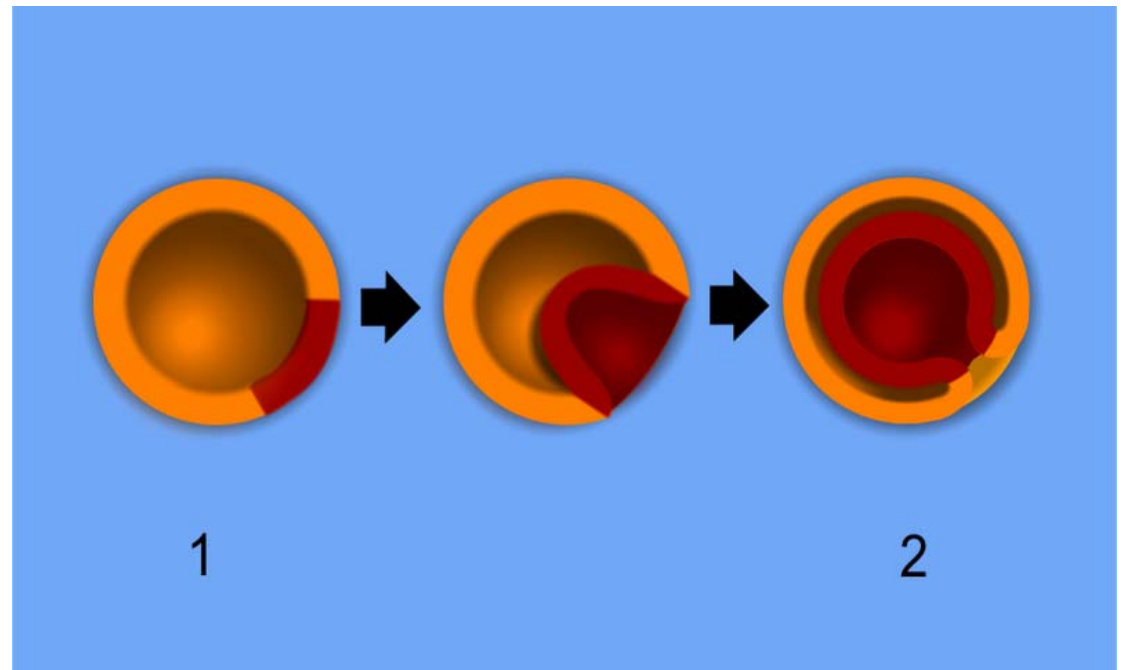
blastulation



1

2

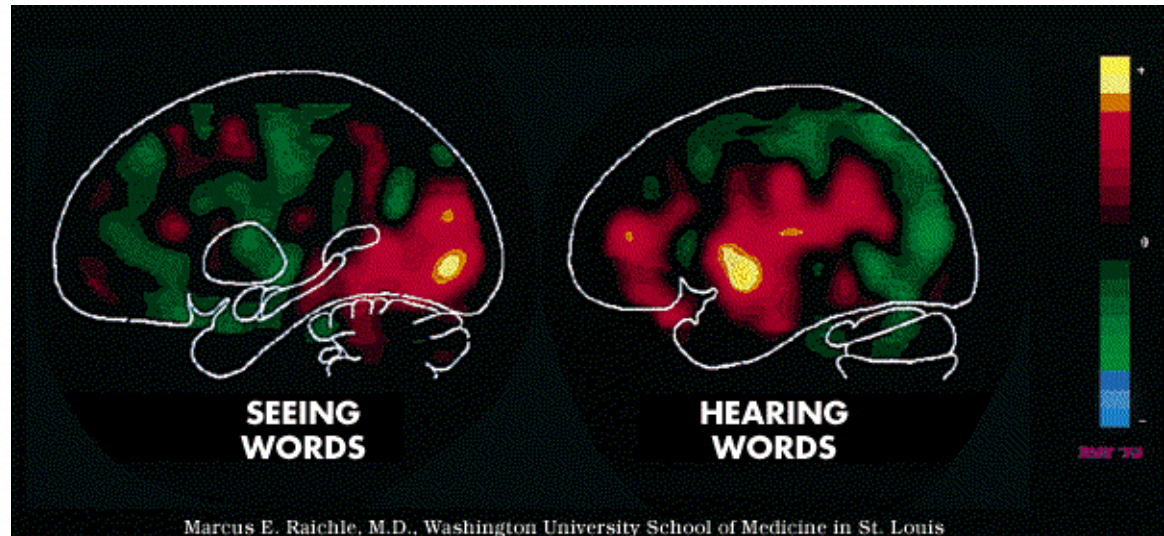
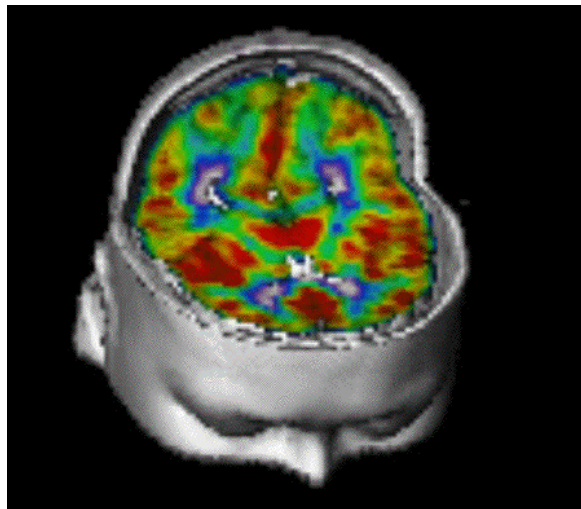
gastrulation



1

2

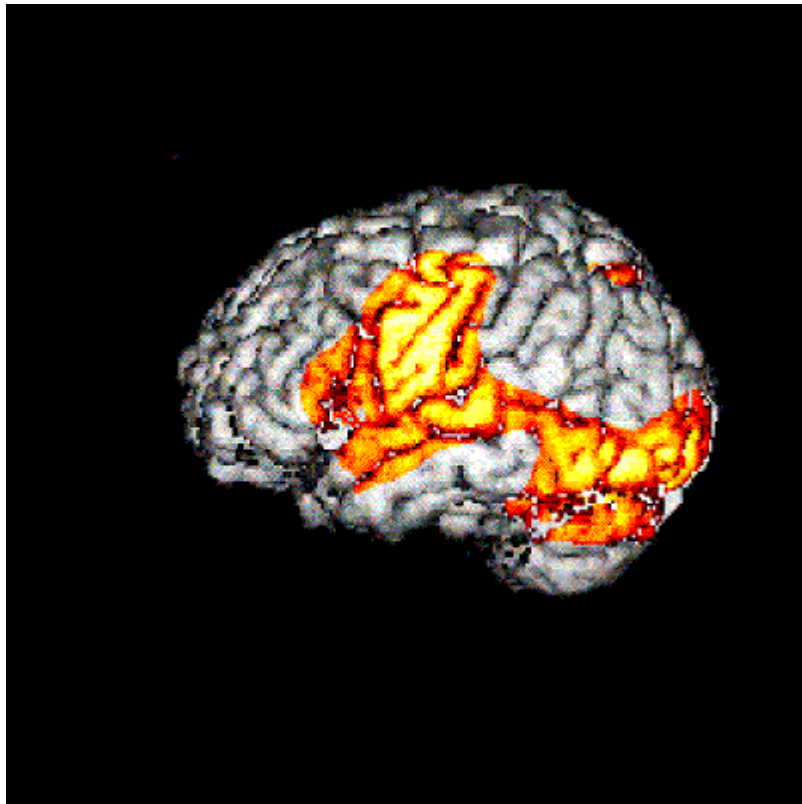
Pattern formation in
animal development



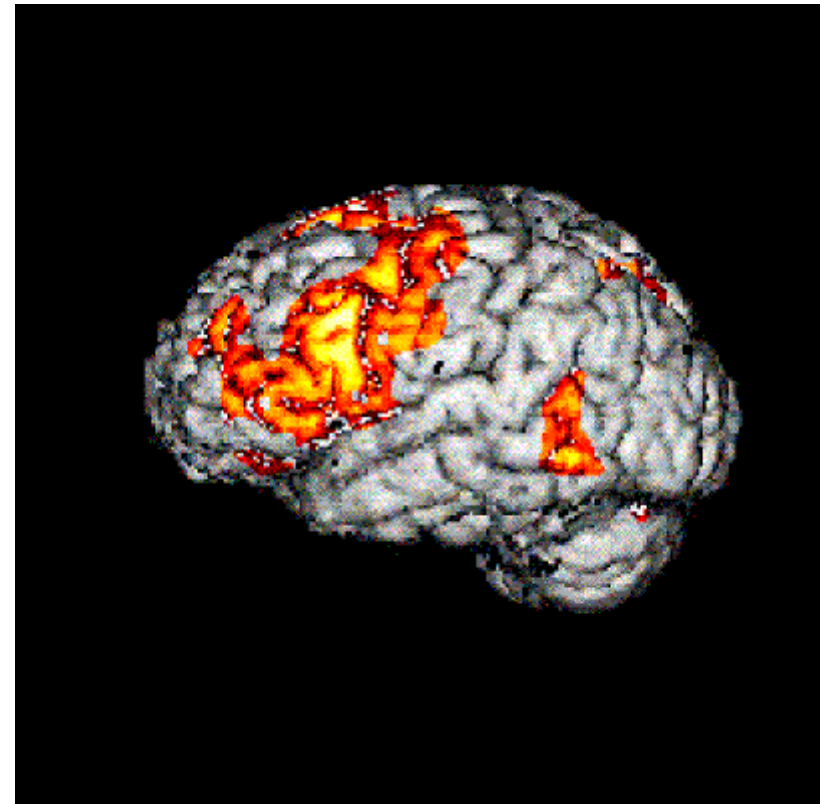
The PET scan on the left shows two areas of the brain (red and yellow) that become particularly active when volunteers read words on a video screen: the primary visual cortex and an additional part of the visual system, both in the back of the left hemisphere. Other brain regions become especially active when subjects hear words through ear-phones, as seen in the PET scan on the right.

Specific pattern formation in the brain correlates with certain activities.

Pictures from the web-page of the Neurobiology Research Unit, Rigshospitalet, Copenhagen, Denmark



reading aloud



silent generation of words

Brain activity relative to the resting state

Pictures from the web-page of the Neurobiology Research Unit, Rigshospitalet, Copenhagen, Denmark

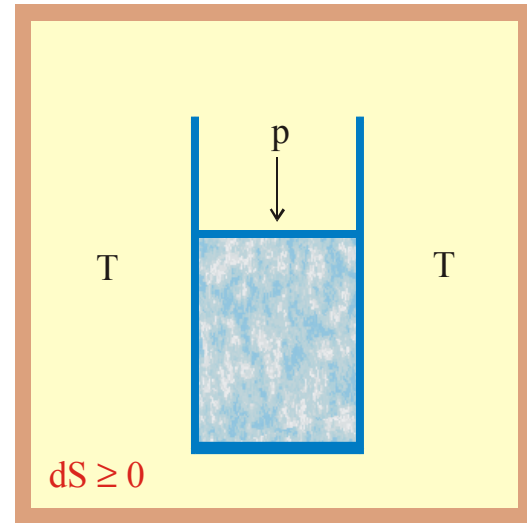
1. Equilibrium structures and dissipative patterns
- 2. Spatio-temporal patterns in chemical reactions**
3. Patterns in development
4. Genetic and metabolic networks
5. Patterns in neurobiology

$$dS \geq 0$$

Isolated system

$$U = \text{const.}, V = \text{const.},$$

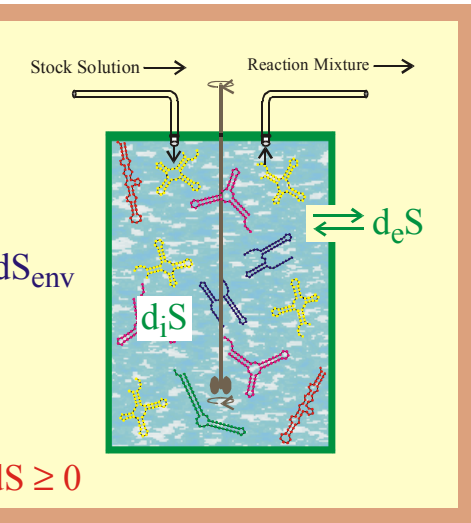
$$dS \geq 0$$



Closed system

$$T = \text{const.}, p = \text{const.},$$

$$dG = dU - pdV - TdS \leq 0$$



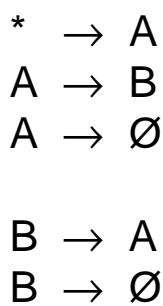
Open system

$$dS = dS_{\text{env}} + dS \geq 0$$

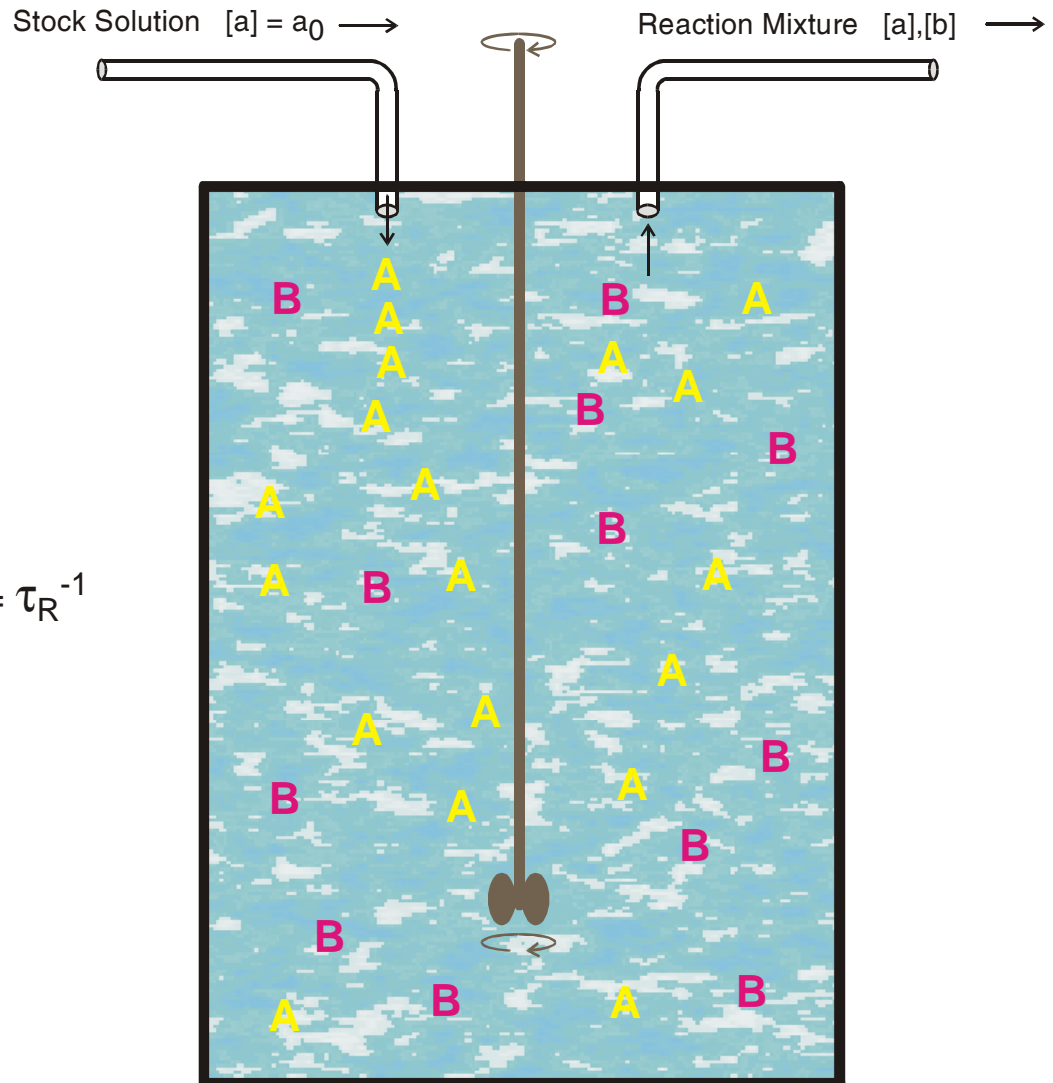
$$dS = d_i S + d_e S$$

$$d_i S \geq 0$$

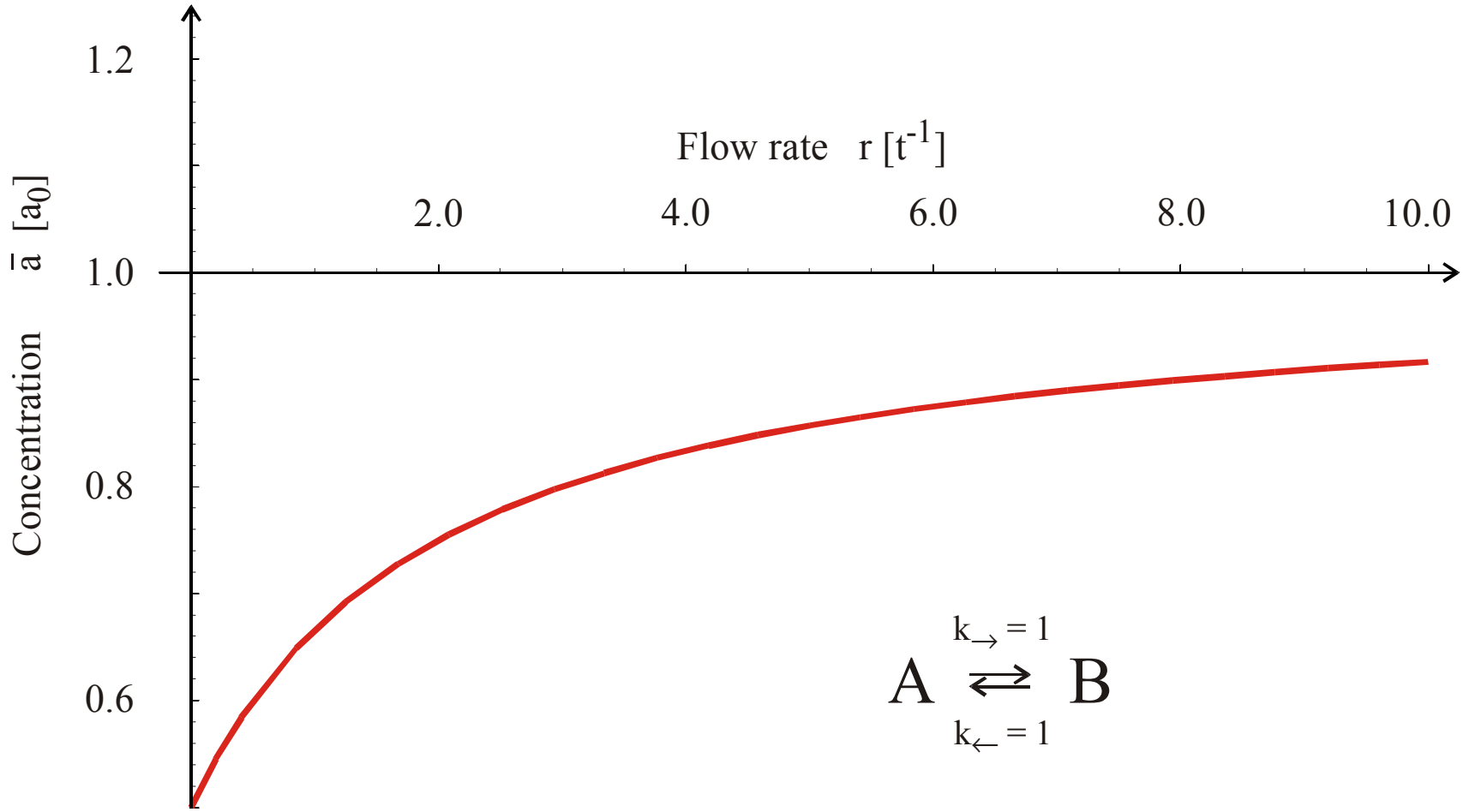
Entropy changes in different thermodynamic systems



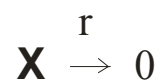
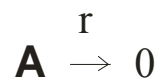
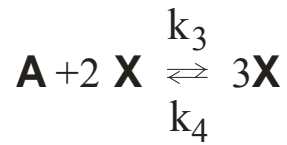
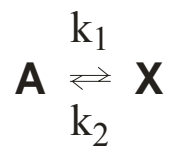
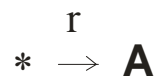
$$\text{Flow rate } r = \tau_R^{-1}$$



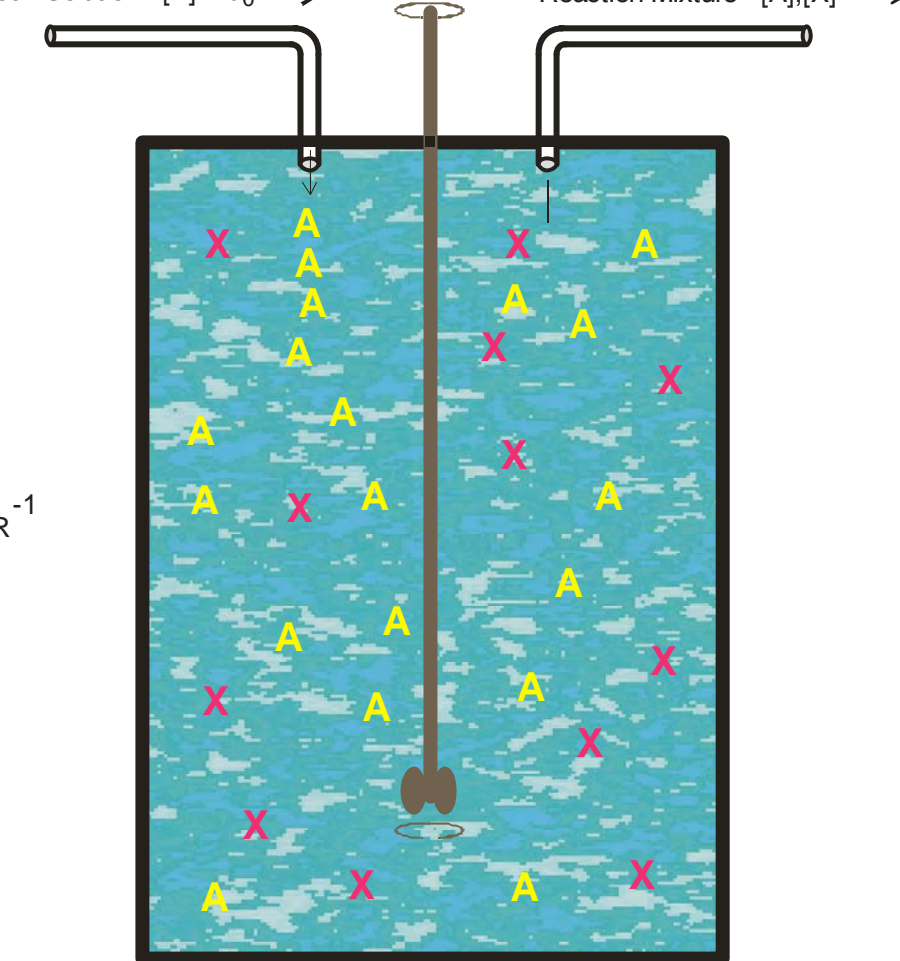
Reactions in the continuously stirred tank reactor (CSTR)

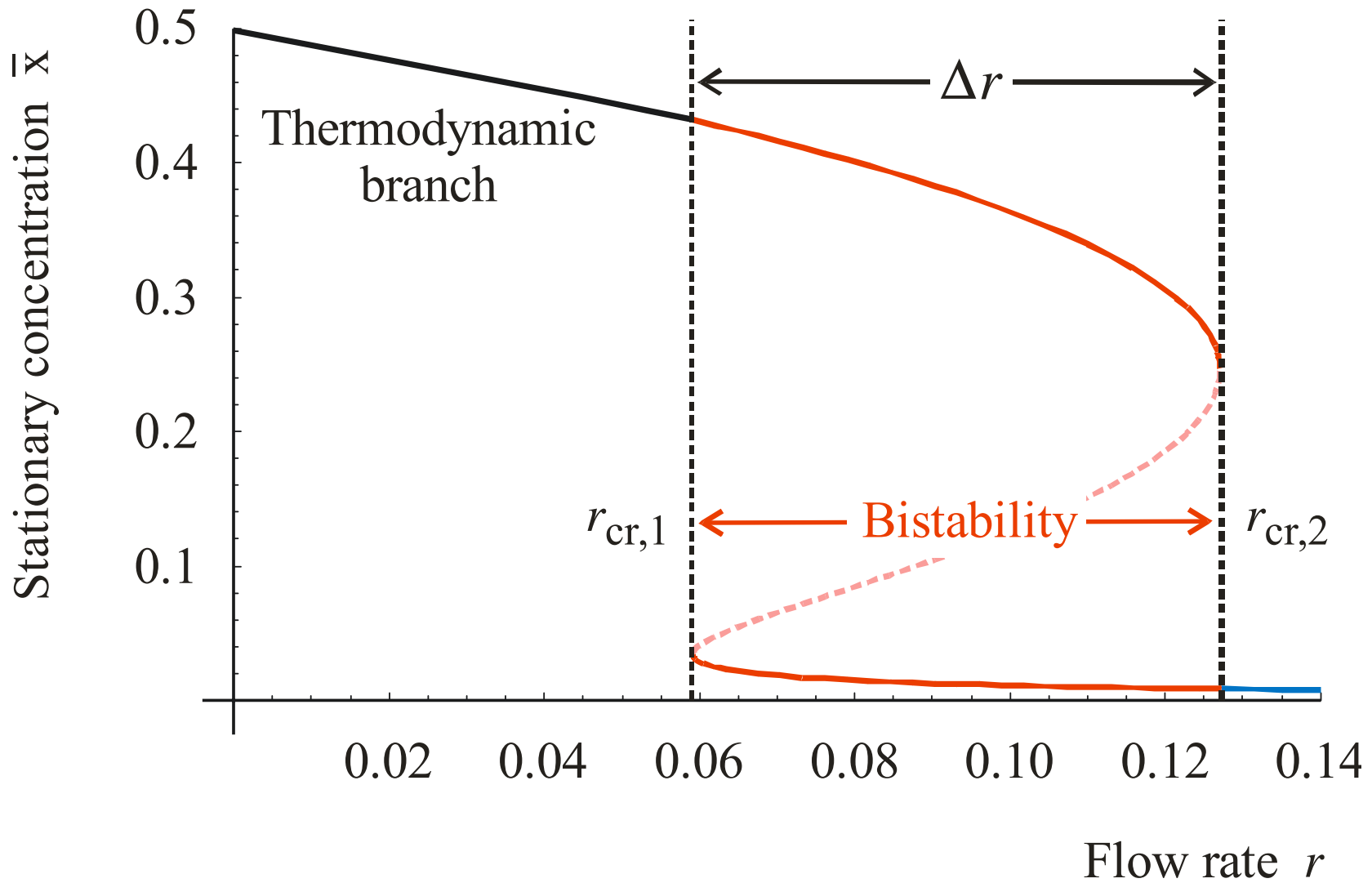


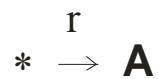
Reversible first order reaction in the flow reactor



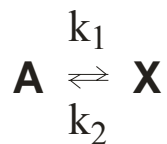
Stock Solution $[A] = a_0 \longrightarrow$ Reaction Mixture $[A], [X] \longrightarrow$



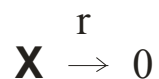
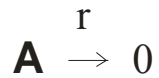
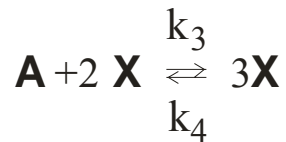


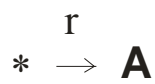


Kinetic differential equations:

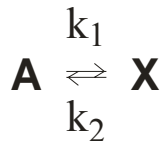


$$\frac{d[\mathbf{A}]}{dt} = \frac{da}{dt} = r(a_0 - a) - (k_1 + k_3 x^2)a + (k_2 + k_4 x^2)x$$



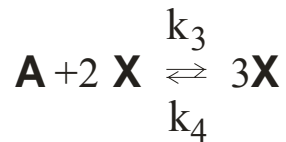


Kinetic differential equations:



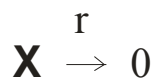
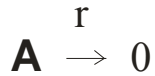
$$\frac{d[\mathbf{A}]}{dt} = \frac{da}{dt} = r(a_0 - a) - (k_1 + k_3 x^2)a + (k_2 + k_4 x^2)x$$

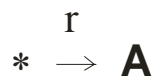
$$\frac{d[\mathbf{X}]}{dt} = \frac{dx}{dt} = -r x + (k_1 + k_3 x^2)a - (k_2 + k_4 x^2)x$$



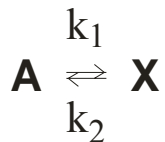
Steady states:

$$\bar{x}^3(k_3 + k_4) - \bar{x}^2 k_3 a_0 + \bar{x}(k_1 + k_2 + r) - k_1 a_0 = 0$$



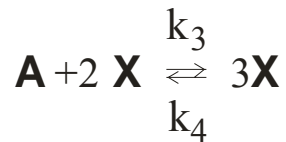


Kinetic differential equations:



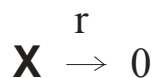
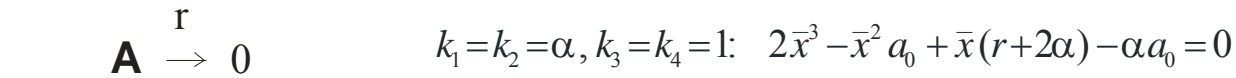
$$\frac{d[\mathbf{A}]}{dt} = \frac{da}{dt} = r(a_0 - a) - (k_1 + k_3 x^2)a + (k_2 + k_4 x^2)x$$

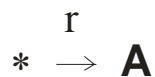
$$\frac{d[\mathbf{X}]}{dt} = \frac{dx}{dt} = -r x + (k_1 + k_3 x^2)a - (k_2 + k_4 x^2)x$$



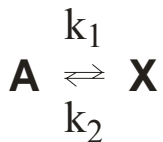
Steady states:

$$\bar{x}^3(k_3 + k_4) - \bar{x}^2 k_3 a_0 + \bar{x}(k_1 + k_2 + r) - k_1 a_0 = 0$$



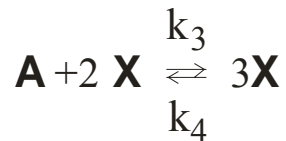


Kinetic differential equations:



$$\frac{d[\mathbf{A}]}{dt} = \frac{da}{dt} = r(a_0 - a) - (k_1 + k_3 x^2)a + (k_2 + k_4 x^2)x$$

$$\frac{d[\mathbf{X}]}{dt} = \frac{dx}{dt} = -r x + (k_1 + k_3 x^2)a - (k_2 + k_4 x^2)x$$



Steady states:

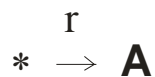
$$\bar{x}^3(k_3 + k_4) - \bar{x}^2 k_3 a_0 + \bar{x}(k_1 + k_2 + r) - k_1 a_0 = 0$$



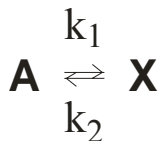
$$k_1 = k_2 = \alpha, k_3 = k_4 = 1: 2\bar{x}^3 - \bar{x}^2 a_0 + \bar{x}(r + 2\alpha) - \alpha a_0 = 0$$

Polynomial discriminant of the cubic equation:

$$216 D = r^3 + r^2 \left(6\alpha - \frac{a_0^2}{8} \right) + r(12\alpha^2 - 5\alpha a_0^2) + 8\alpha^3 + 4\alpha^2 a_0^2 + \frac{\alpha a_0^4}{2} = 0$$

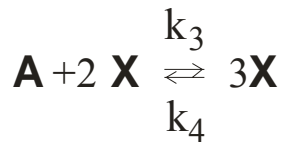


Kinetic differential equations:



$$\frac{d[\mathbf{A}]}{dt} = \frac{da}{dt} = r(a_0 - a) - (k_1 + k_3 x^2)a + (k_2 + k_4 x^2)x$$

$$\frac{d[\mathbf{X}]}{dt} = \frac{dx}{dt} = -r x + (k_1 + k_3 x^2)a - (k_2 + k_4 x^2)x$$



Steady states:

$$\bar{x}^3(k_3 + k_4) - \bar{x}^2 k_3 a_0 + \bar{x}(k_1 + k_2 + r) - k_1 a_0 = 0$$

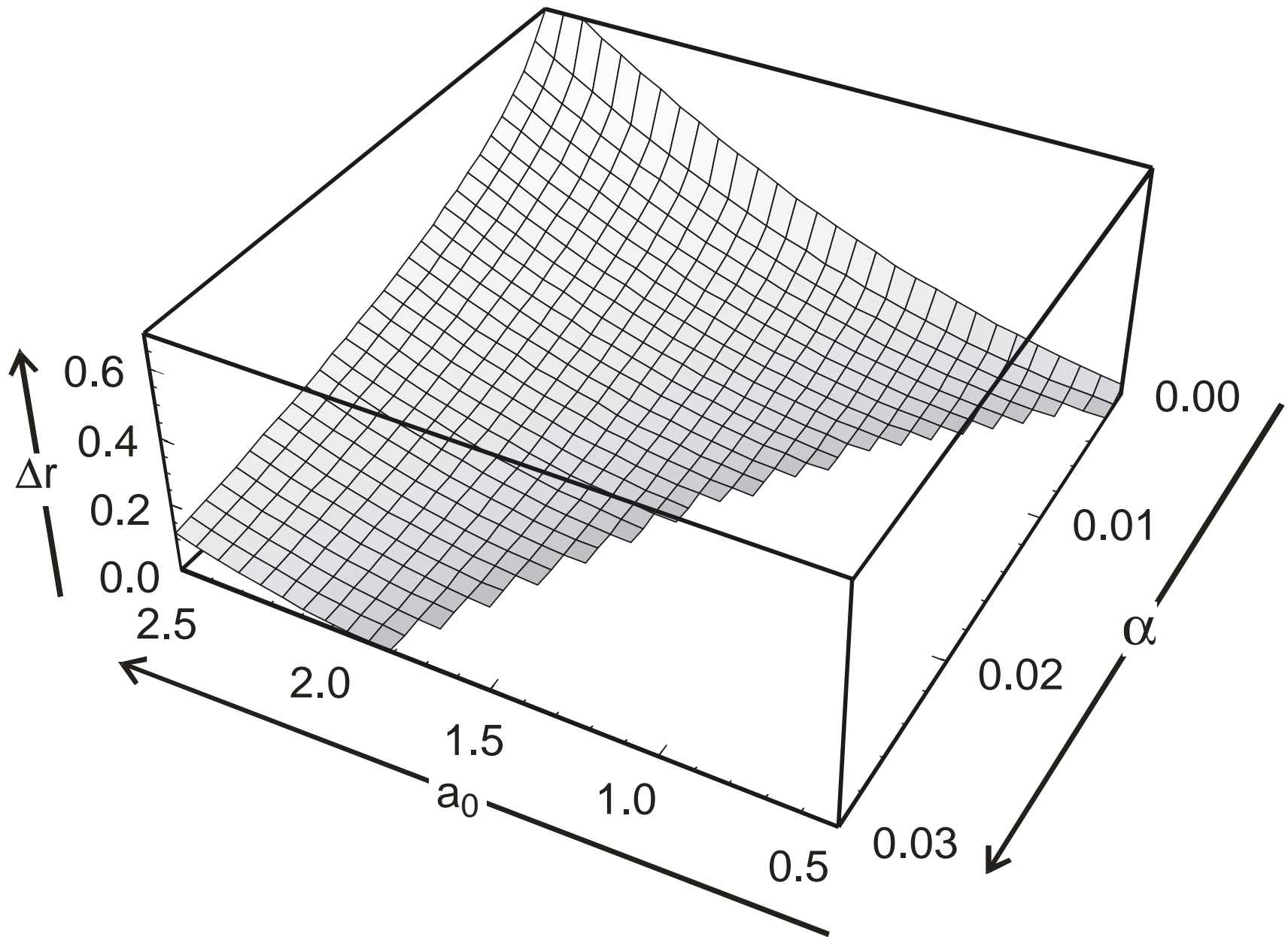


$$k_1 = k_2 = \alpha, k_3 = k_4 = 1: 2\bar{x}^3 - \bar{x}^2 a_0 + \bar{x}(r + 2\alpha) - \alpha a_0 = 0$$

Polynomial discriminant of the cubic equation:

$$216D = r^3 + r^2 \left(6\alpha - \frac{a_0^2}{8}\right) + r(12\alpha^2 - 5\alpha a_0^2) + 8\alpha^3 + 4\alpha^2 a_0^2 + \frac{\alpha a_0^4}{2} = 0$$

$D < 0$: 3 roots r_1, r_2 , and r_3 , 2 are positive $\Rightarrow \Delta r = r_1 - r_2$



Range of hysteresis as a function of the parameters a_0 and α

$$\frac{dc_i}{dt} = F_i(c_1, c_2, \dots, c_n); \quad i=1, 2, \dots, n \quad \text{chemical reaction}$$

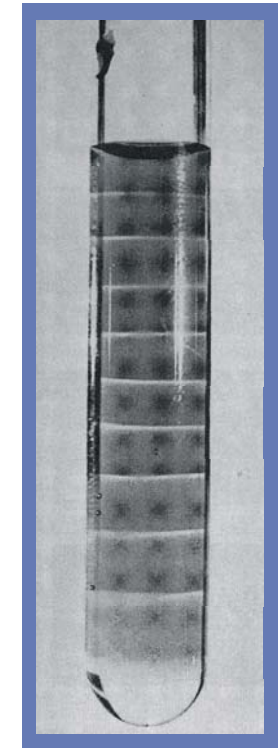
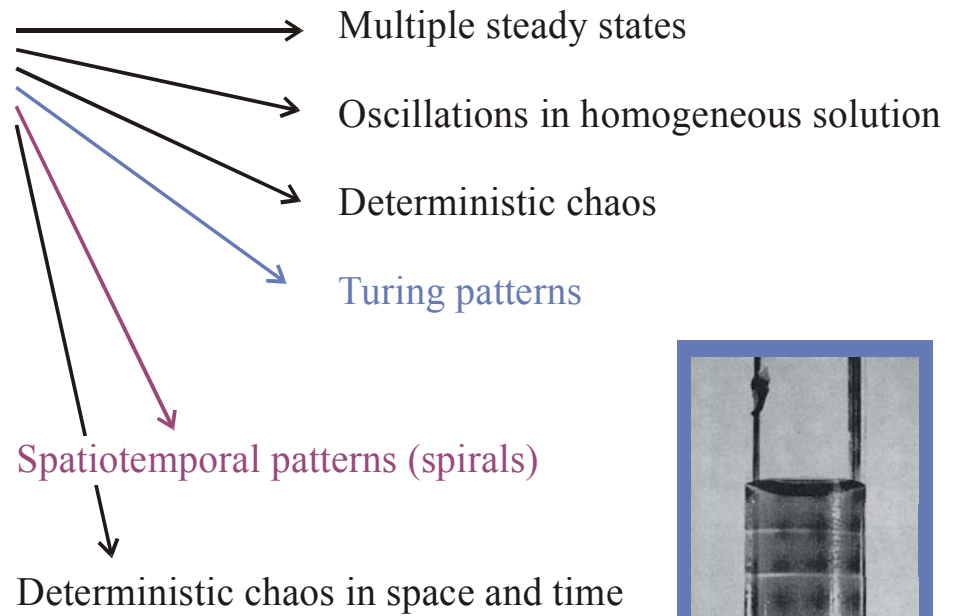
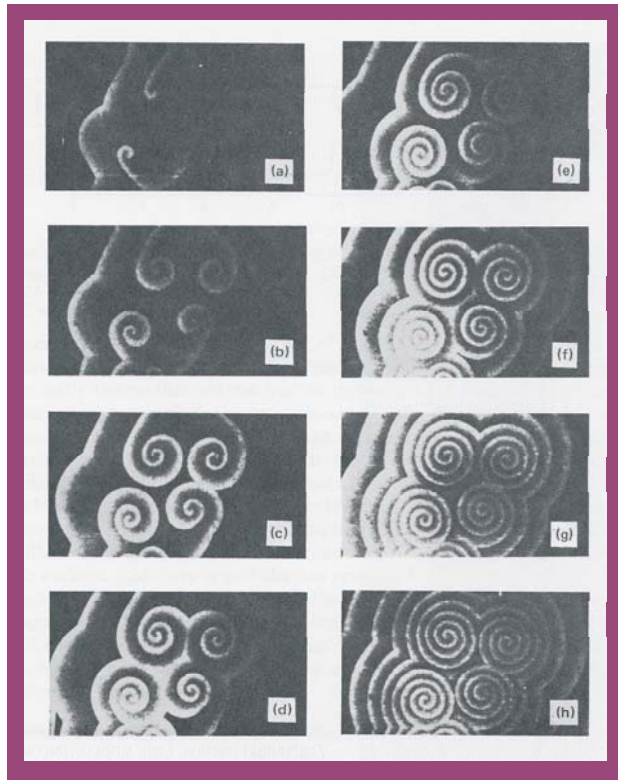
$$\frac{\partial c_i}{\partial t} = D_i \Delta c_i \quad \text{diffusion}$$

$$\Delta c_i = \left(\frac{\partial^2 c_i}{\partial x^2} + \frac{\partial^2 c_i}{\partial y^2} + \frac{\partial^2 c_i}{\partial z^2} \right)$$

$$\frac{\partial c_i}{\partial t} = D_i \Delta c_i + F_i(c_1, c_2, \dots, c_n); \quad i=1, 2, \dots, n \quad \text{reaction-diffusion}$$

Autocatalytic third order reactions

Direct, $\mathbf{A} + 2 \mathbf{X} \rightarrow 3 \mathbf{X}$, or hidden in the reaction mechanism
(Belousov-Zhabotinskii reaction).



Pattern formation in autocatalytic third order reactions

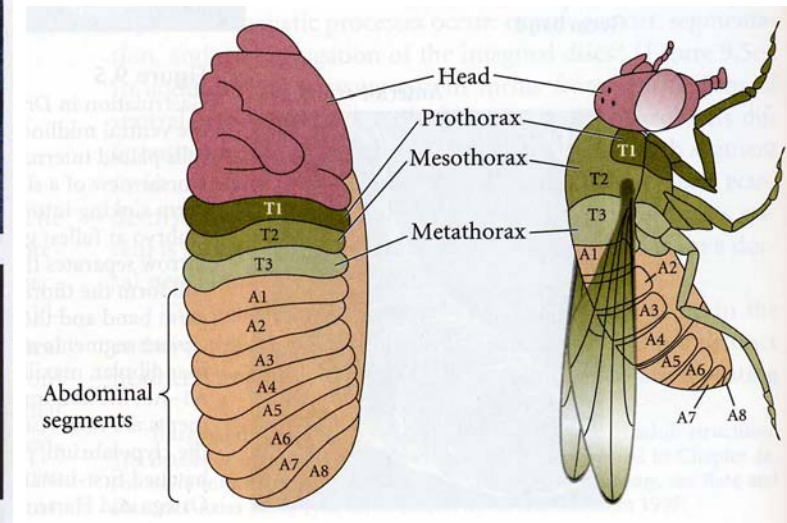
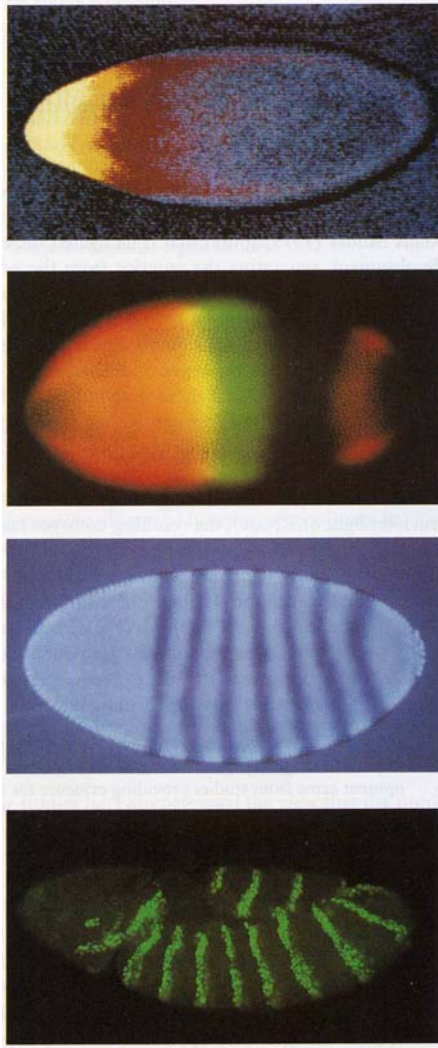
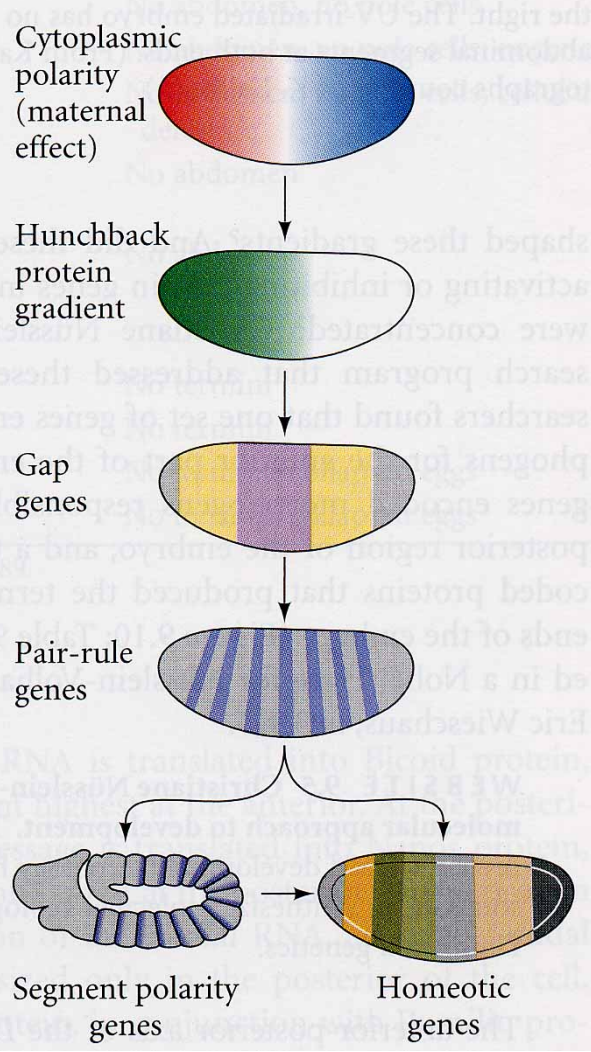
G.Nicolis, I.Prigogine. *Self-Organization in Nonequilibrium Systems. From Dissipative Structures to Order through Fluctuations*. John Wiley, New York 1977

1. Equilibrium structures and dissipative patterns
2. Spatio-temporal patterns in chemical reactions
- 3. Patterns in development**
4. Genetic and metabolic networks
5. Patterns in neurobiology

Gierer–Meinhardt model

$$\frac{\partial a}{\partial t} = D_a \Delta a + \frac{a^2}{(1+ka^2)h} - \mu a + \rho_a$$

$$\frac{\partial h}{\partial t} = D_h \Delta h + \rho a^2 - \nu h + \rho_h; \quad D_h > D_a$$



Cascades, $A \Rightarrow B \Rightarrow C \Rightarrow \dots$, and networks of genetic control

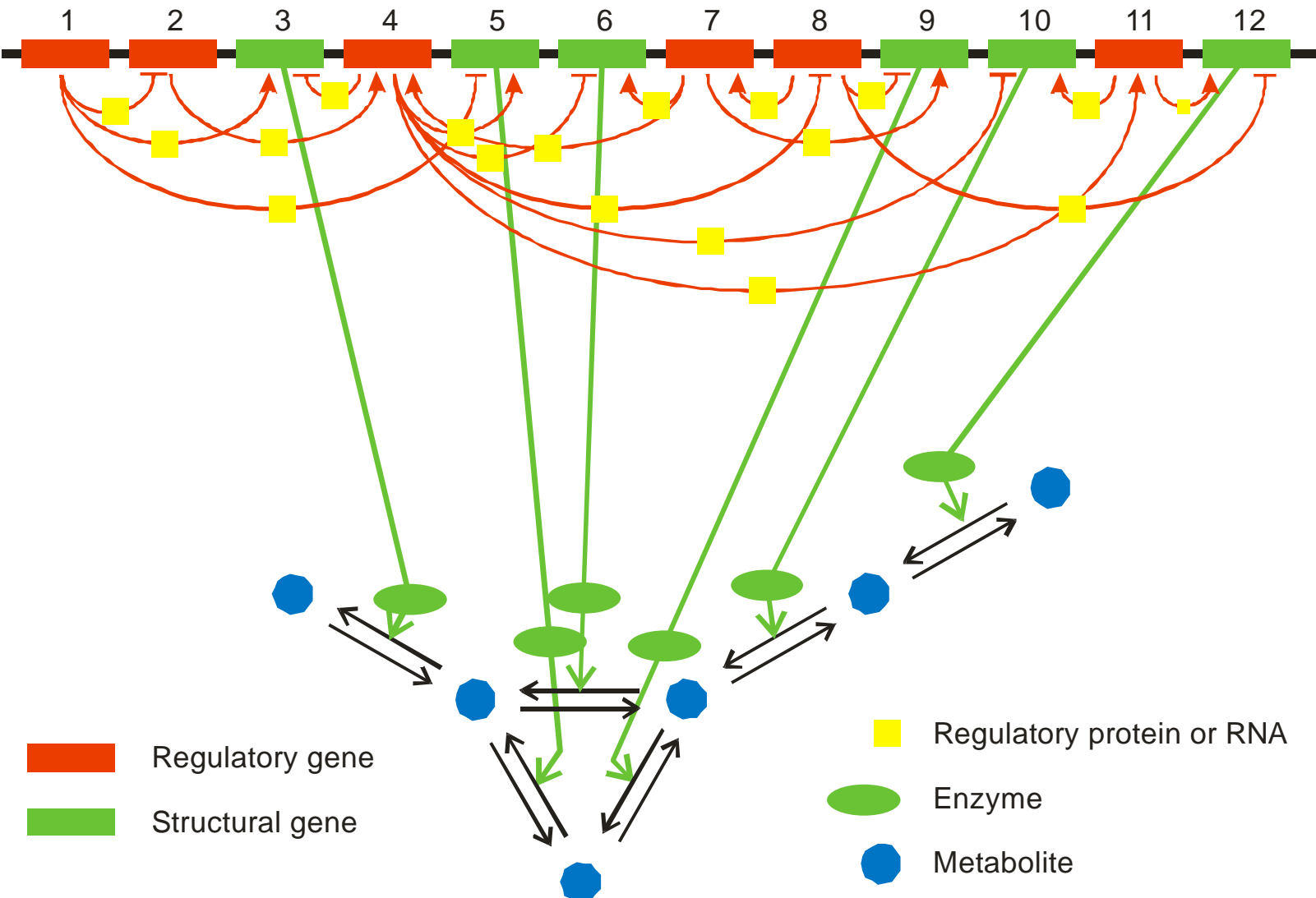
Turing pattern resulting from reaction-diffusion equation ?

Intercellular communication creating positional information

Development of the fruit fly *drosophila melanogaster*: Genetics, experiment, and imago

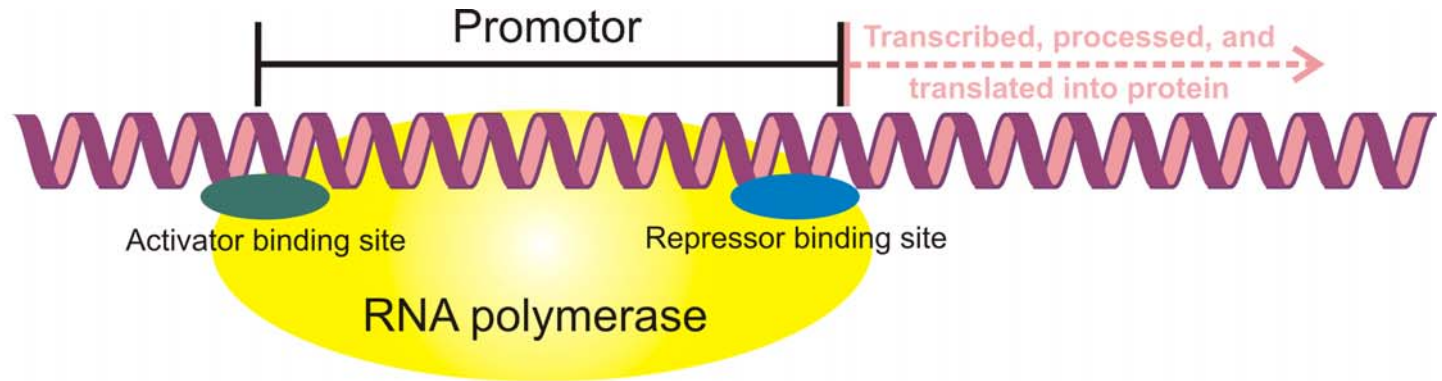
1. Equilibrium structures and dissipative patterns
2. Spatio-temporal patterns in chemical reactions
3. Patterns in development
- 4. Genetic and metabolic networks**
5. Patterns in neurobiology

A model genome with 12 genes

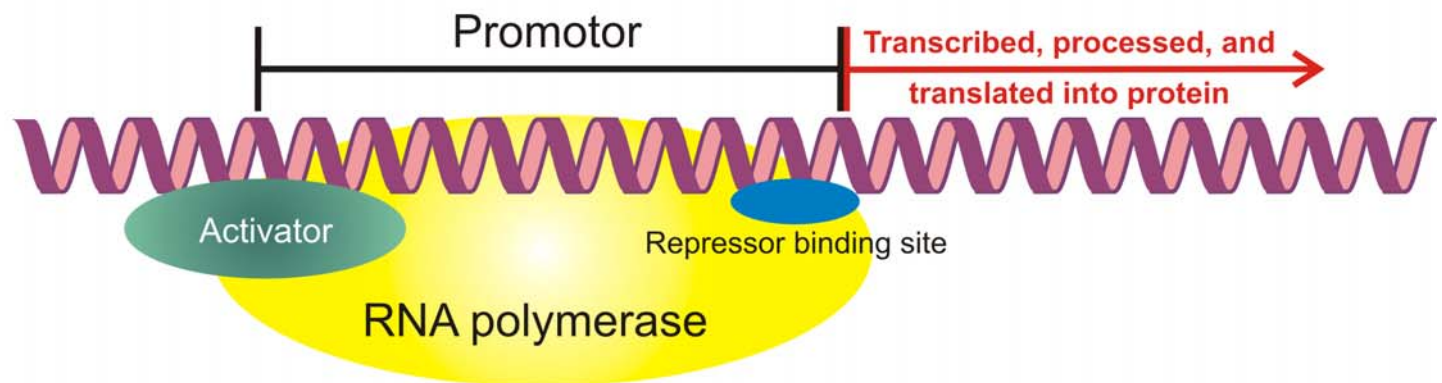


Sketch of a genetic and metabolic network

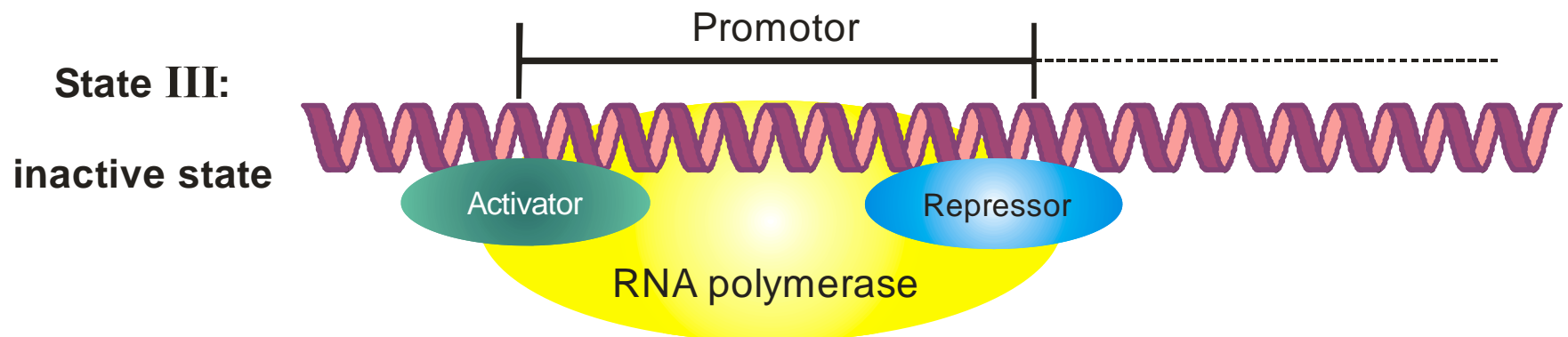
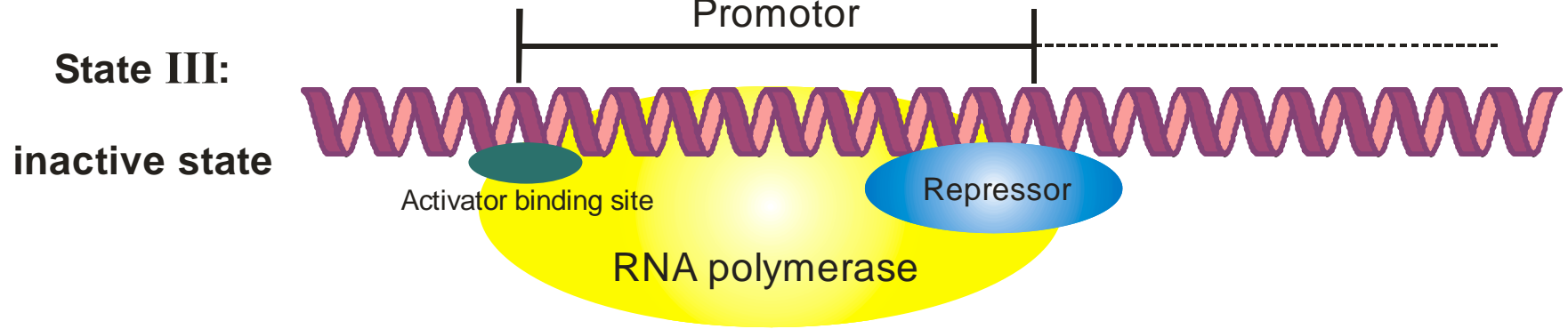
State I:
basal state



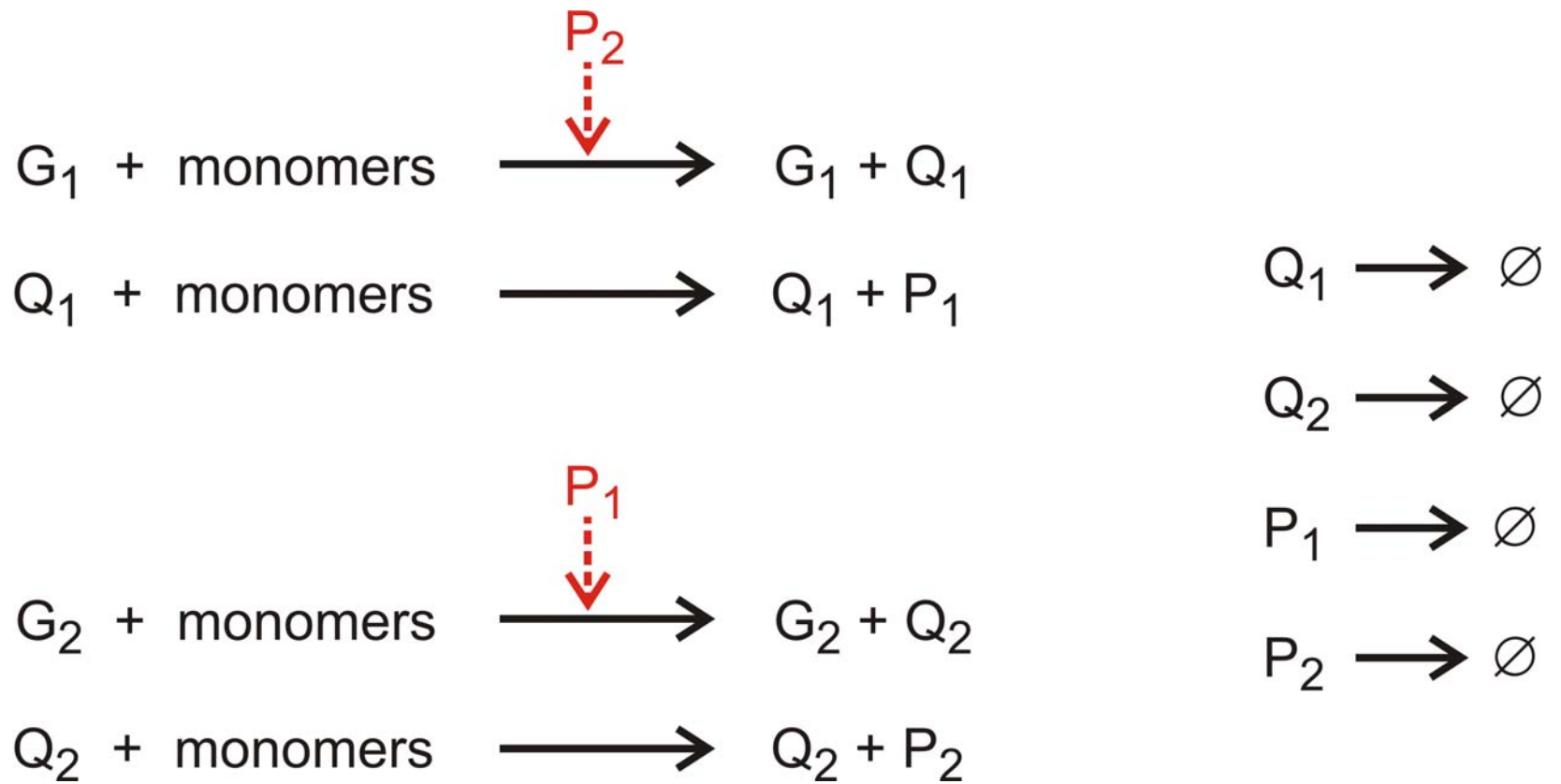
State II:
active state



Active states of gene regulation



Inactive states of gene regulation

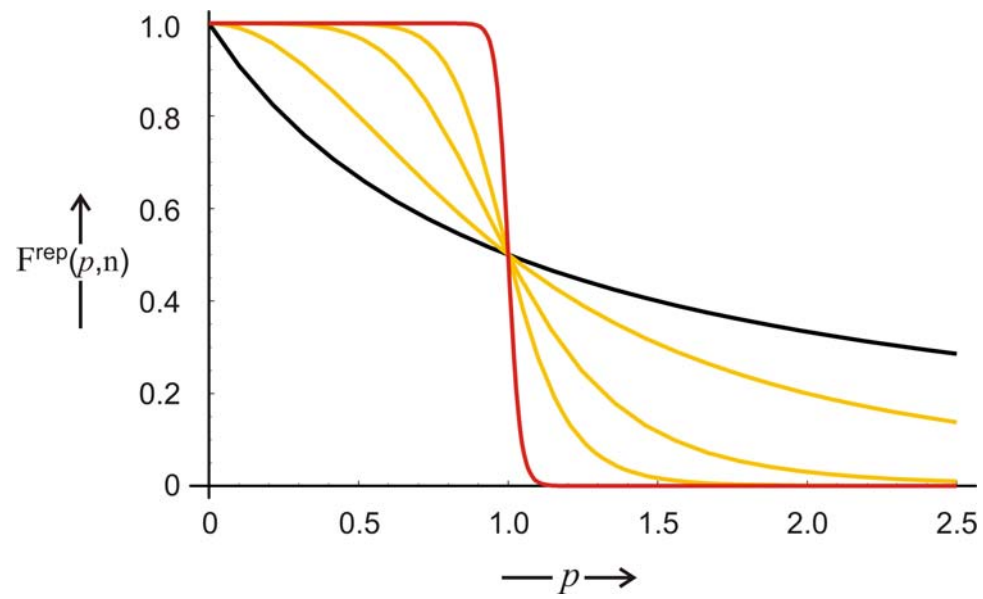
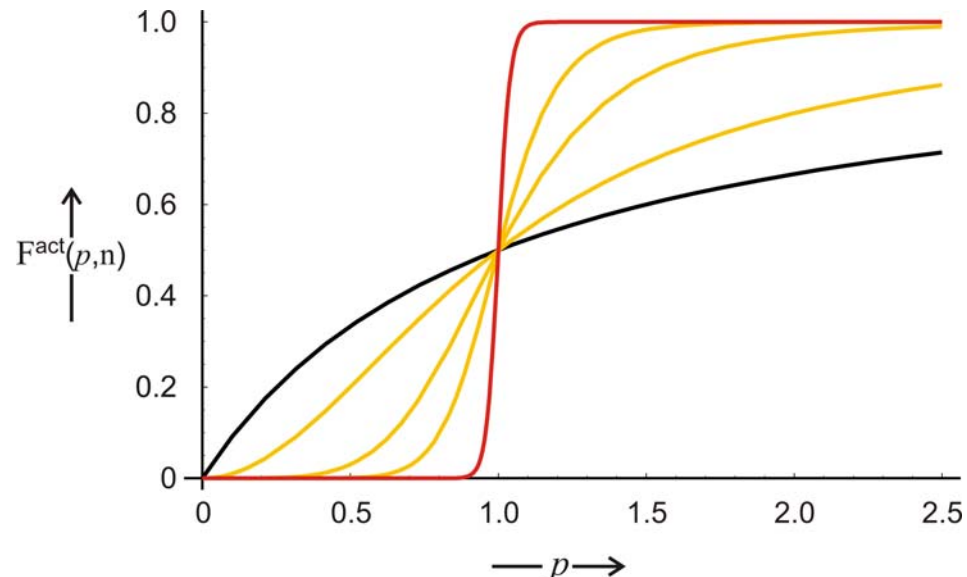


Cross-regulation of two genes

Activation: $F_i(p_j) = \frac{p_j^n}{K + p_j^n}$

Repression: $F_i(p_j) = \frac{K}{K + p_j^n}$

$$i, j = 1, 2$$



Gene regulatory binding functions

$$[G_1] = [G_2] = g_0 = \text{const.}$$

$$[Q_1] = q_1, [Q_2] = q_2,$$

$$[P_1] = p_1, [P_2] = p_2$$

$$\text{Activation: } F_i(p_j) = \frac{p_j^n}{K + p_j^n}$$

$$\text{Repression: } F_i(p_j) = \frac{K}{K + p_j^n}$$
$$i, j = 1, 2$$

$$\frac{dq_1}{dt} = k_1^Q F_1(p_2) - d_1^Q q_1$$

$$\frac{dq_2}{dt} = k_2^Q F_2(p_1) - d_2^Q q_2$$

$$\frac{dp_1}{dt} = k_1^P q_1 - d_2^P p_1$$

$$\frac{dp_2}{dt} = k_2^P q_2 - d_2^P p_2$$

$$\text{Stationary points: } \bar{p}_1 - \vartheta_1 F_1(\vartheta_2 F_2(\bar{p}_1)) = 0, \bar{p}_2 = \vartheta_2 F_2(\bar{p}_1)$$

$$\vartheta_1 = \frac{k_1^Q k_1^P}{d_1^Q d_1^P}, \vartheta_2 = \frac{k_2^Q k_2^P}{d_2^Q d_2^P}$$

Qualitative analysis of cross-regulation of two genes: **Stationary points**

$$\mathbf{A} = \left\{ a_{ij} = \frac{\partial \dot{x}_i}{\partial x_j} \right\} = \begin{pmatrix} Q_D & Q_K \\ P_D & P_K \end{pmatrix} = \begin{pmatrix} -d_1^Q & 0 & k_1^Q \frac{\partial F_1}{\partial p_1} & k_1^Q \frac{\partial F_1}{\partial p_2} \\ 0 & -d_2^Q & k_2^Q \frac{\partial F_2}{\partial p_1} & k_2^Q \frac{\partial F_2}{\partial p_2} \\ k_1^P & 0 & -d_1^P & 0 \\ 0 & k_2^P & 0 & -d_2^P \end{pmatrix}$$

$$Q_D \cdot P_K = P_K \cdot Q_D \quad \text{and hence} \quad \begin{vmatrix} Q_D & Q_K \\ P_K & P_D \end{vmatrix} = |Q_D \cdot P_D - Q_K \cdot P_K|$$

$$\Gamma(\bar{p}_1, \bar{p}_2) = - \begin{vmatrix} 0 & \frac{\partial F_1}{\partial p_2} \\ \frac{\partial F_2}{\partial p_1} & 0 \end{vmatrix} = \frac{\partial F_1}{\partial p_2} \cdot \frac{\partial F_2}{\partial p_1}$$

Qualitative analysis of cross-regulation of two genes: **Jacobian matrix**

$$(\varepsilon+d_1^{\rm Q})(\varepsilon+d_2^{\rm Q})(\varepsilon+d_1^{\rm P})(\varepsilon+d_2^{\rm P})+D=0$$

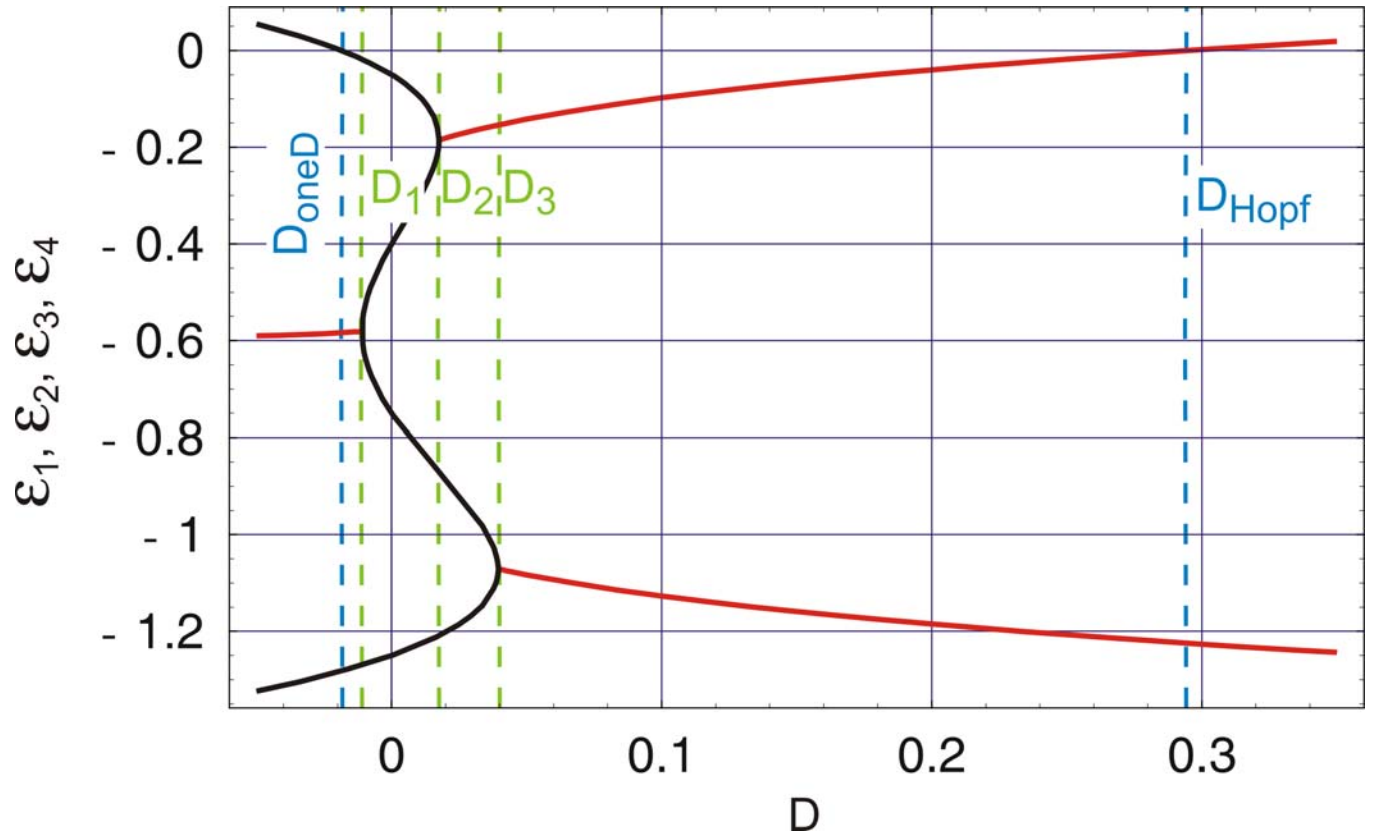
$$D=-k_1^{\rm Q}k_2^{\rm Q}k_1^{\rm P}k_2^{\rm P}\Gamma(\overline{p}_1,\overline{p}_2)$$

$$\Gamma(\overline{p}_1,\overline{p}_2) = - \begin{vmatrix} 0 & \frac{\partial F_1}{\partial p_2} \\ \frac{\partial F_2}{\partial p_1} & 0 \end{vmatrix} = \frac{\partial F_1}{\partial p_2}.\frac{\partial F_2}{\partial p_1}$$

$$(\varepsilon + d_1^Q)(\varepsilon + d_2^Q)(\varepsilon + d_1^P)(\varepsilon + d_2^P) + D = 0$$

Eigenvalues of the Jacobian of the cross-regulatory two gene system

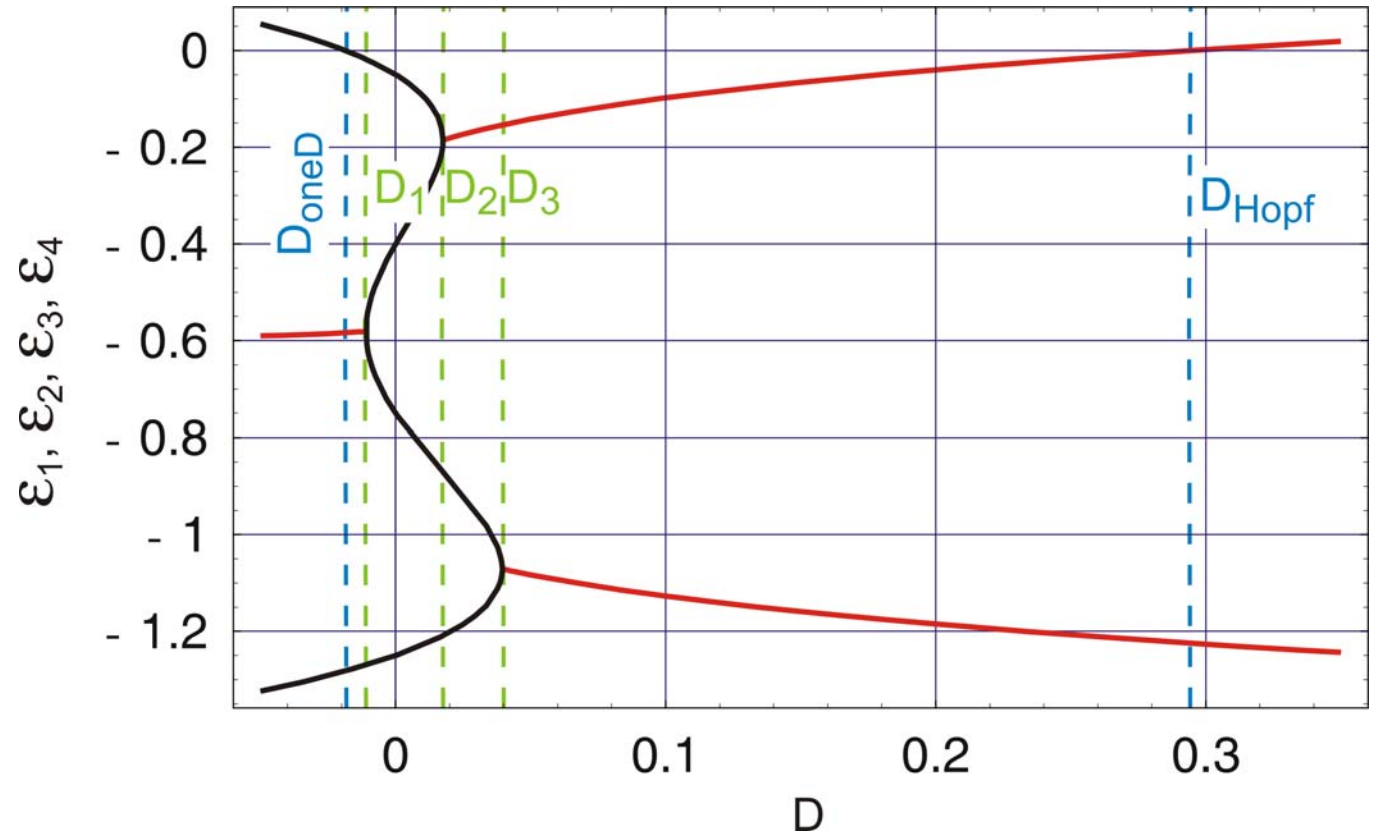
$$D = -k_1^Q k_2^Q k_1^P k_2^P \Gamma(\bar{p}_1, \bar{p}_2)$$



$$(\varepsilon + d_1^Q)(\varepsilon + d_2^Q)(\varepsilon + d_1^P)(\varepsilon + d_2^P) + D = 0$$

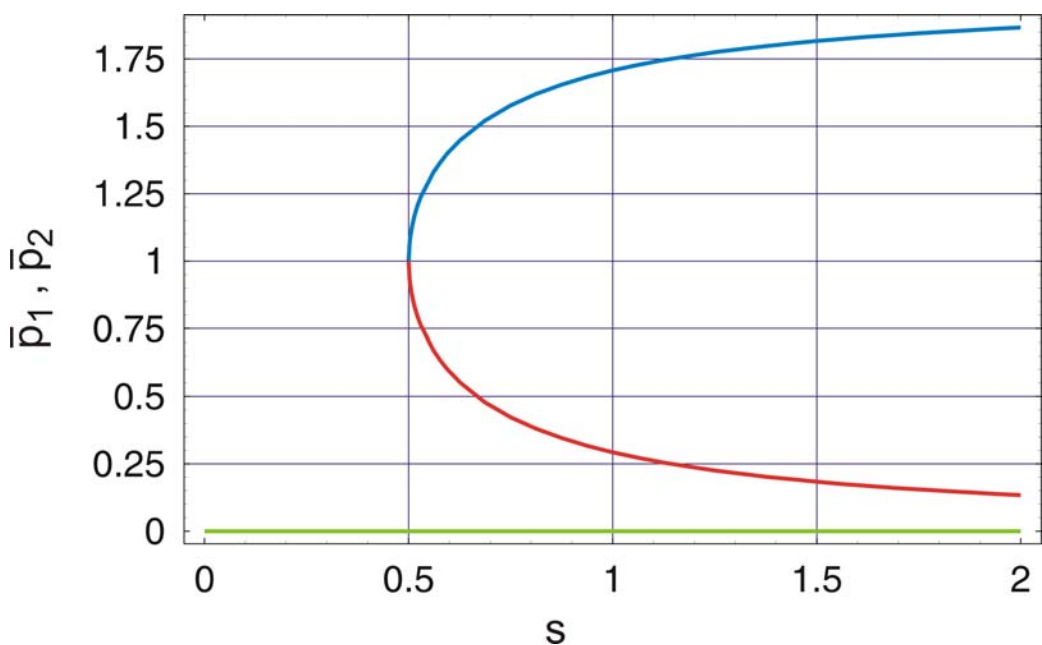
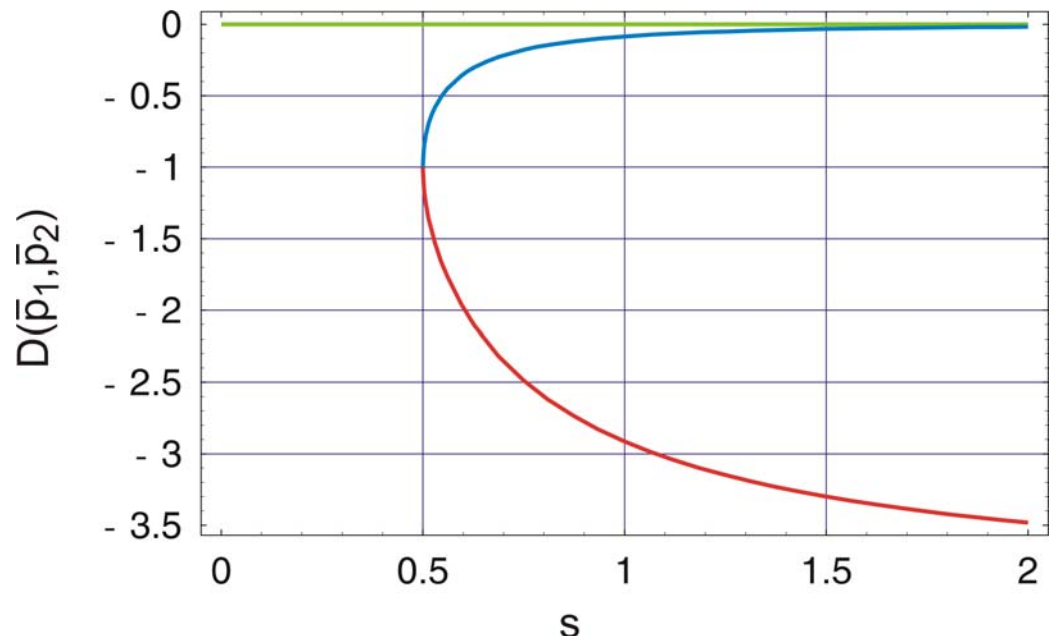
Eigenvalues of the Jacobian of the cross-regulatory two gene system

$$D = -k_1^Q k_2^Q k_1^P k_2^P \Gamma(\bar{p}_1, \bar{p}_2)$$

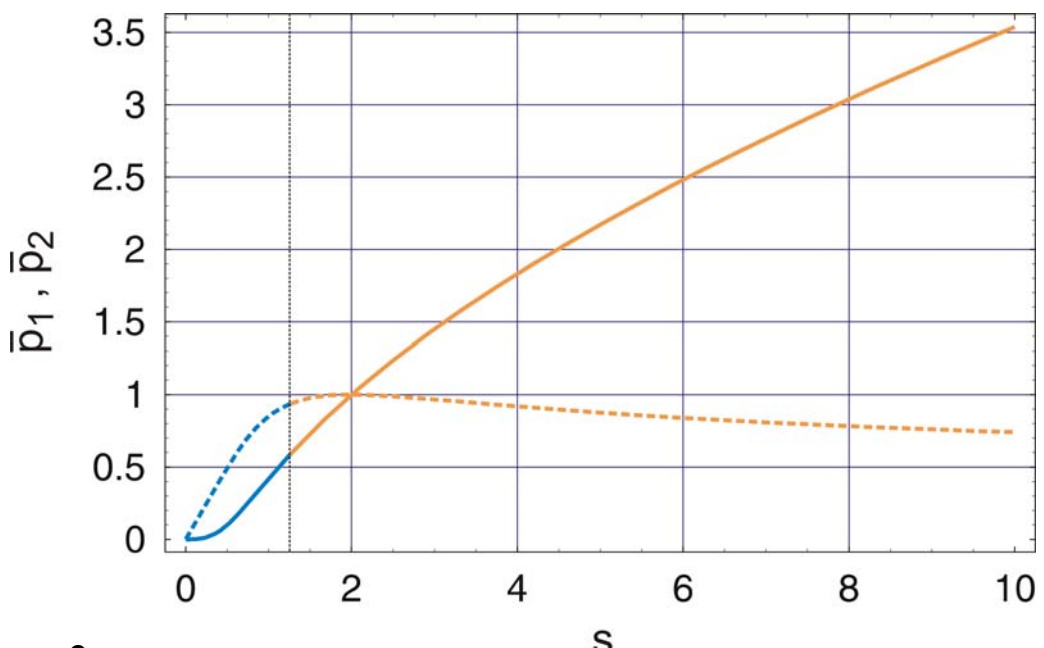
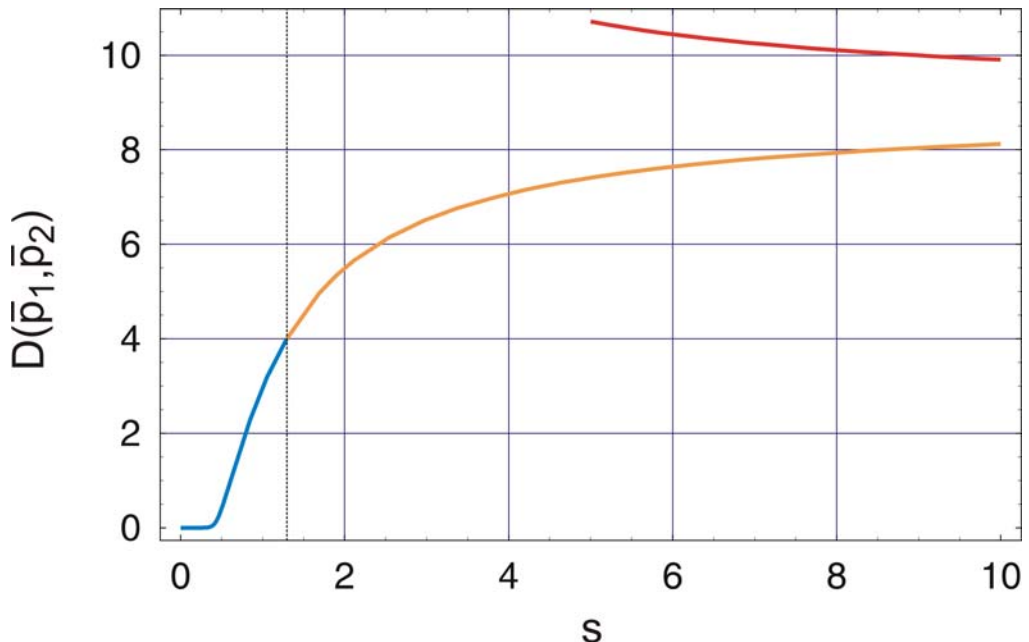


$$D_{\text{OneD}} = -d_1^Q d_2^Q d_1^P d_2^P$$

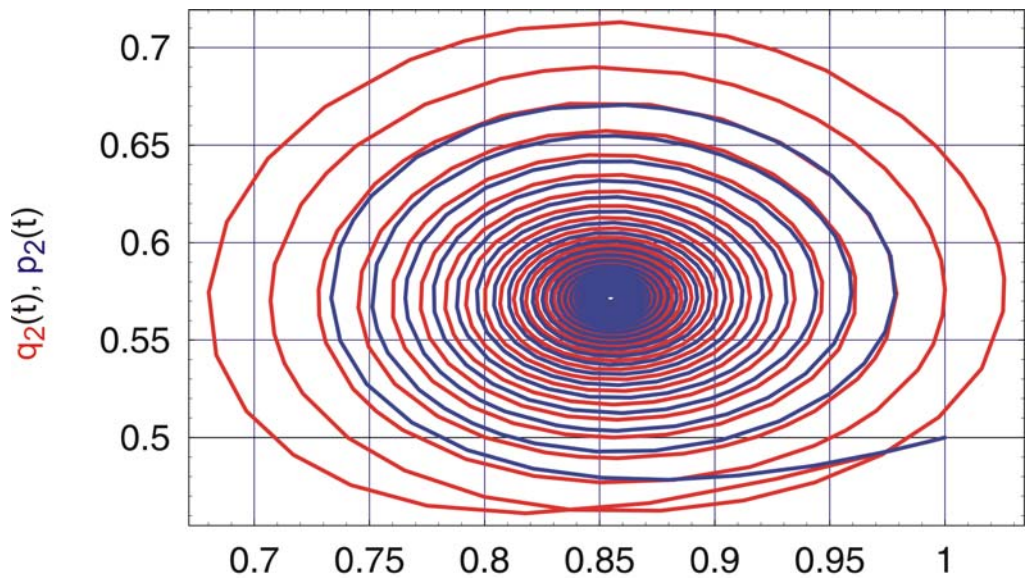
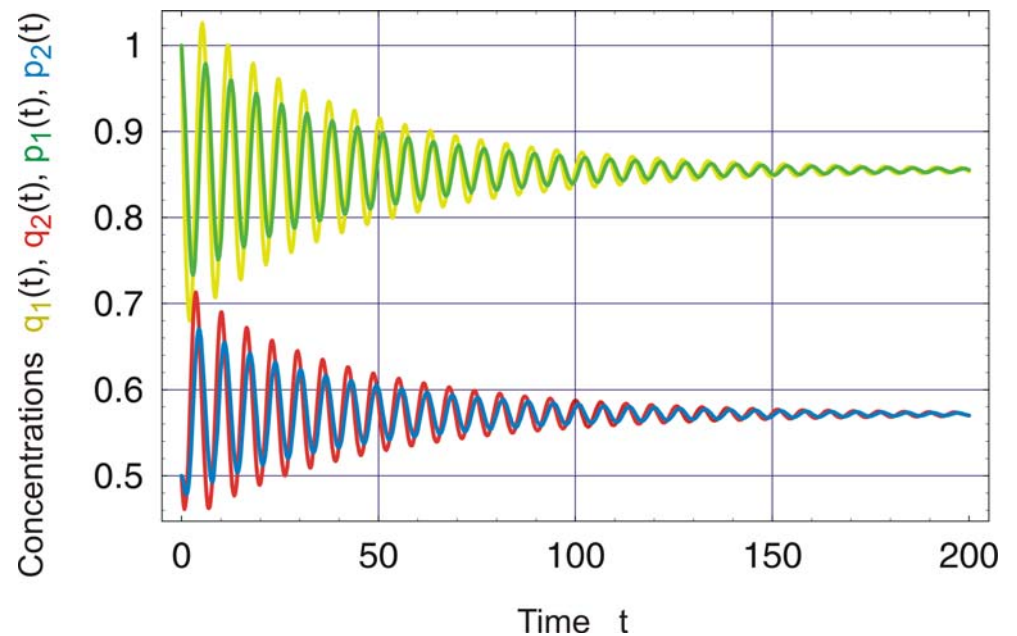
$$D_{\text{Hopf}} = \frac{(d_1^Q + d_2^Q)(d_1^Q + d_1^P)(d_1^Q + d_2^P)(d_2^Q + d_1^P)(d_2^Q + d_2^P)(d_1^P + d_2^P)}{(d_1^Q + d_2^Q + d_1^P + d_2^P)^2}$$



Regulatory dynamics at $D \leq 0$, act.-act., $n=2$

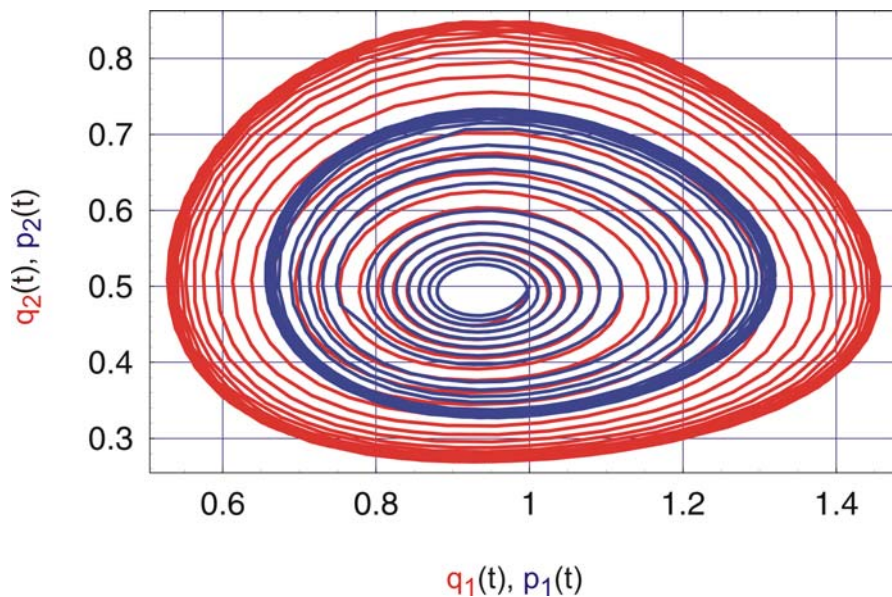
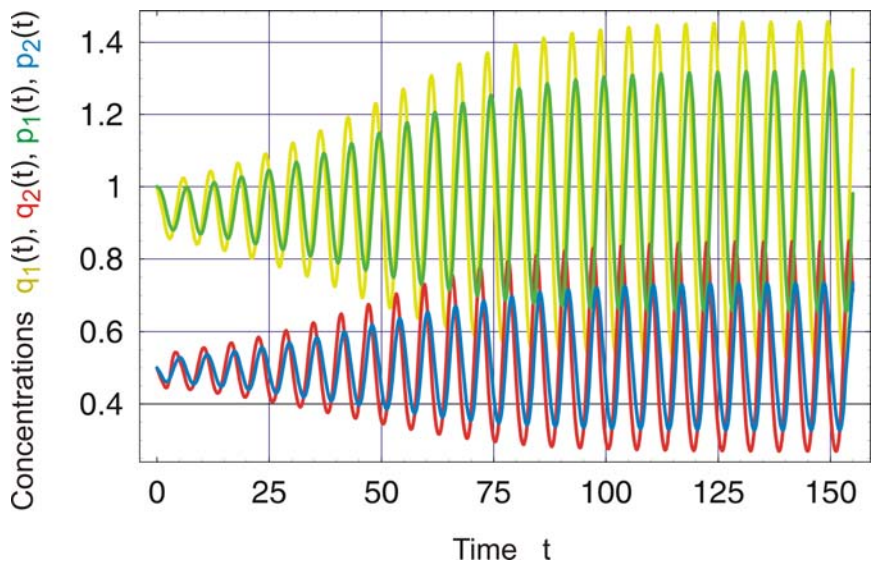
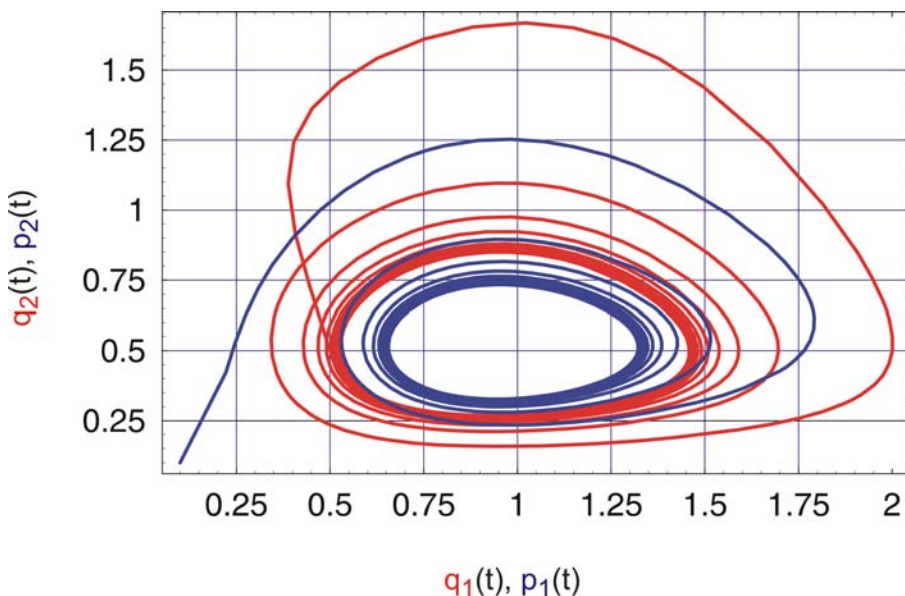
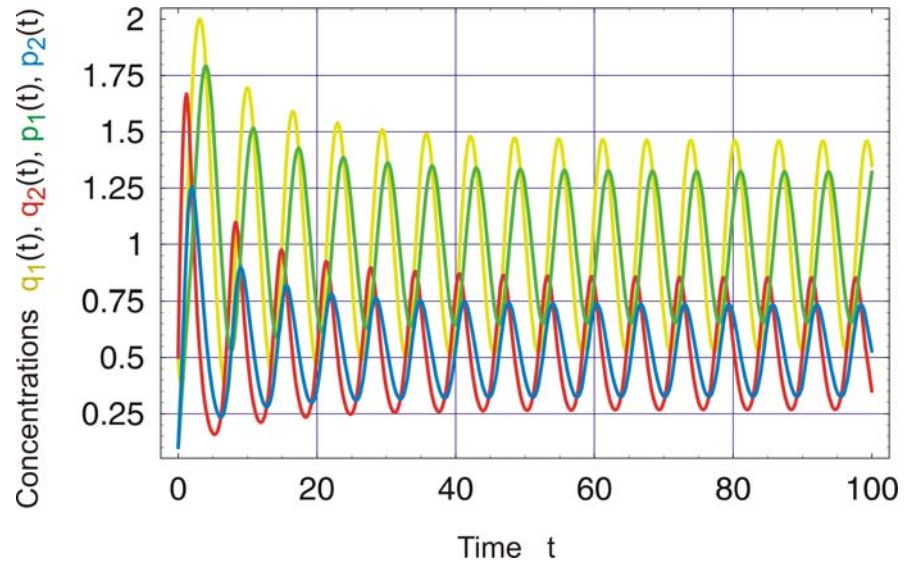


Regulatory dynamics at $D \geq 0$, act.-rep., $n=3$

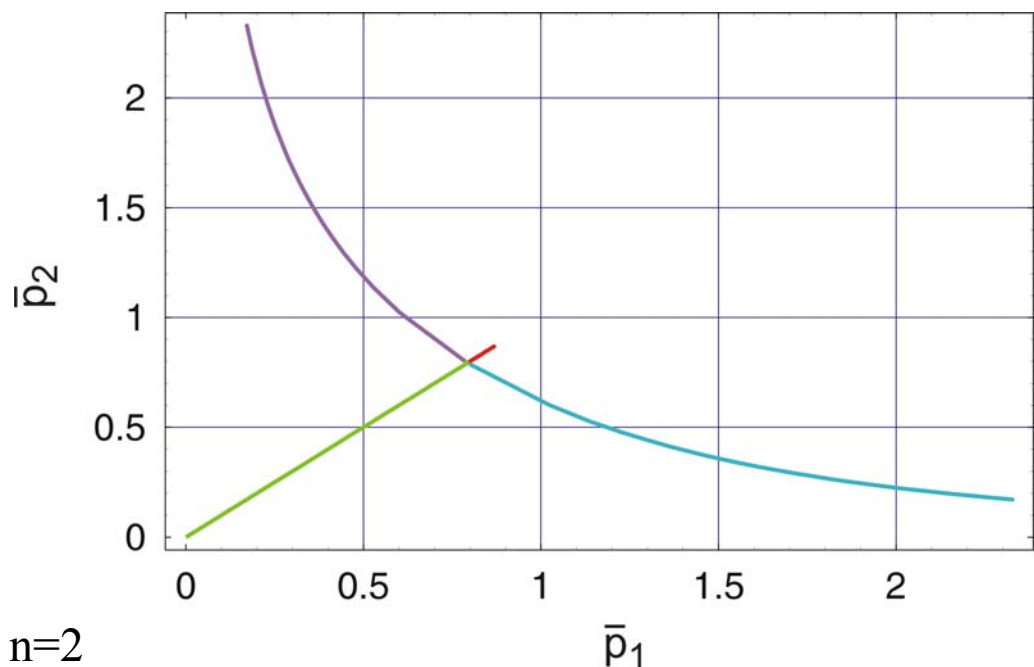
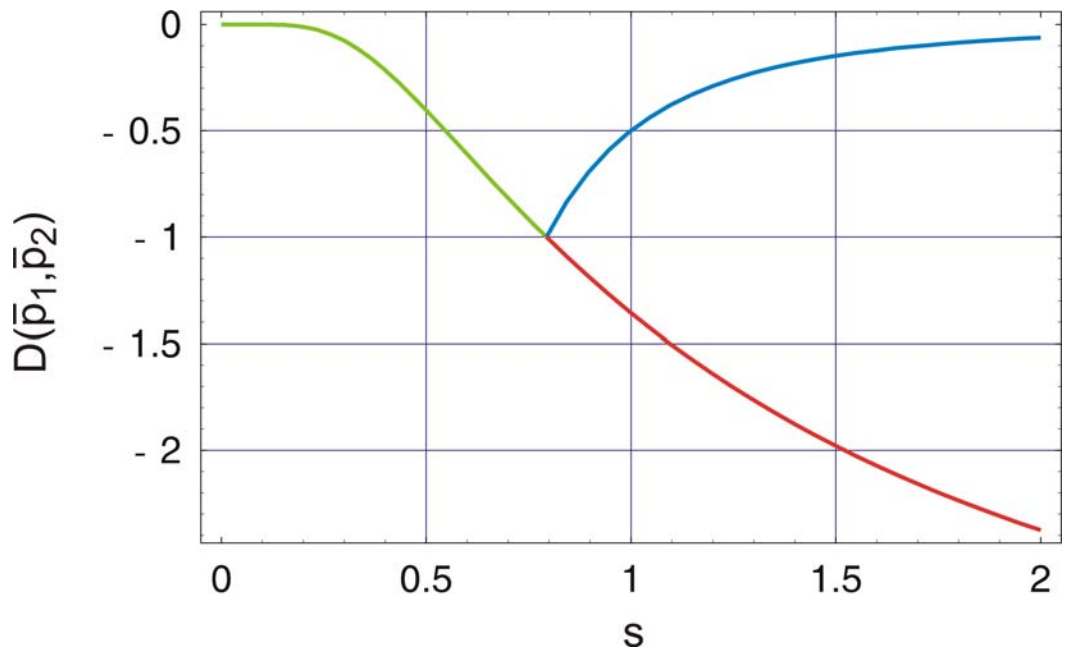


Regulatory dynamics at $D < D_{\text{Hopf}}$, act.-repr., $n=3$

$q_1(t), p_1(t)$

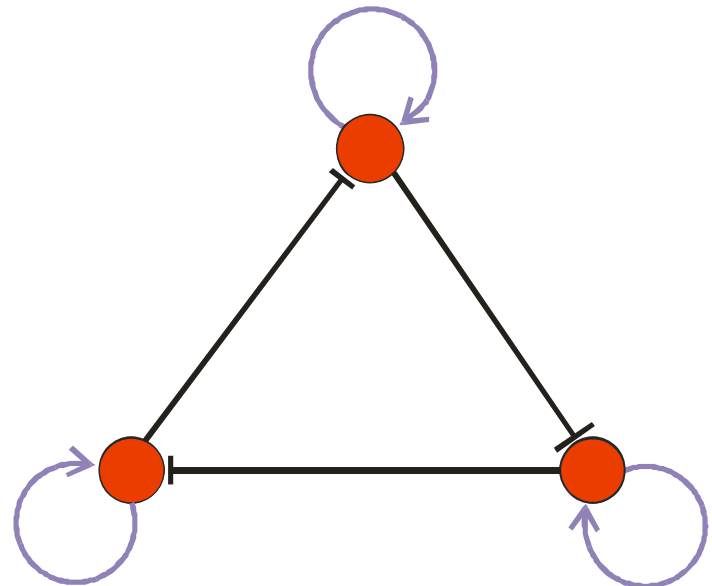
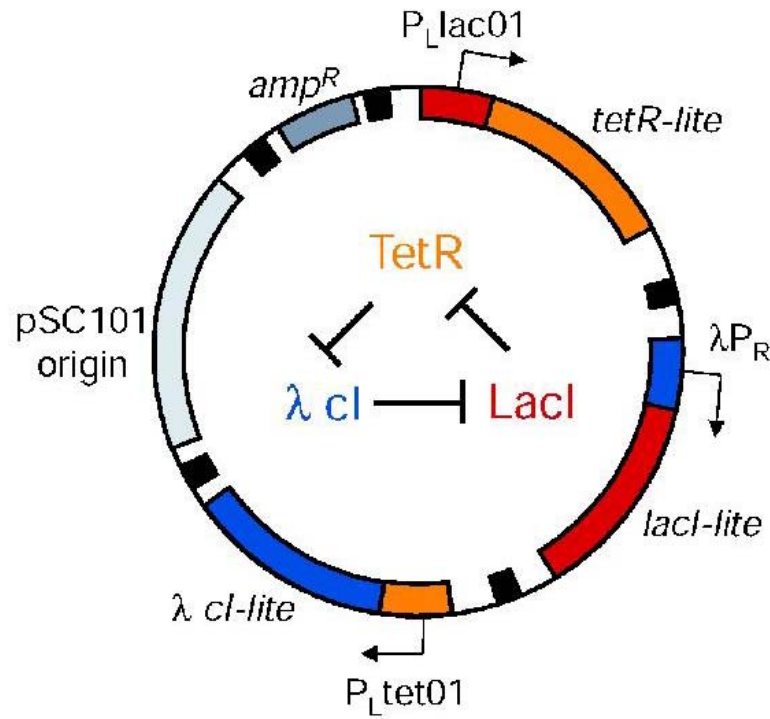


Regulatory dynamics at $D > D_{\text{Hopf}}$, act.-repr., $n=3$



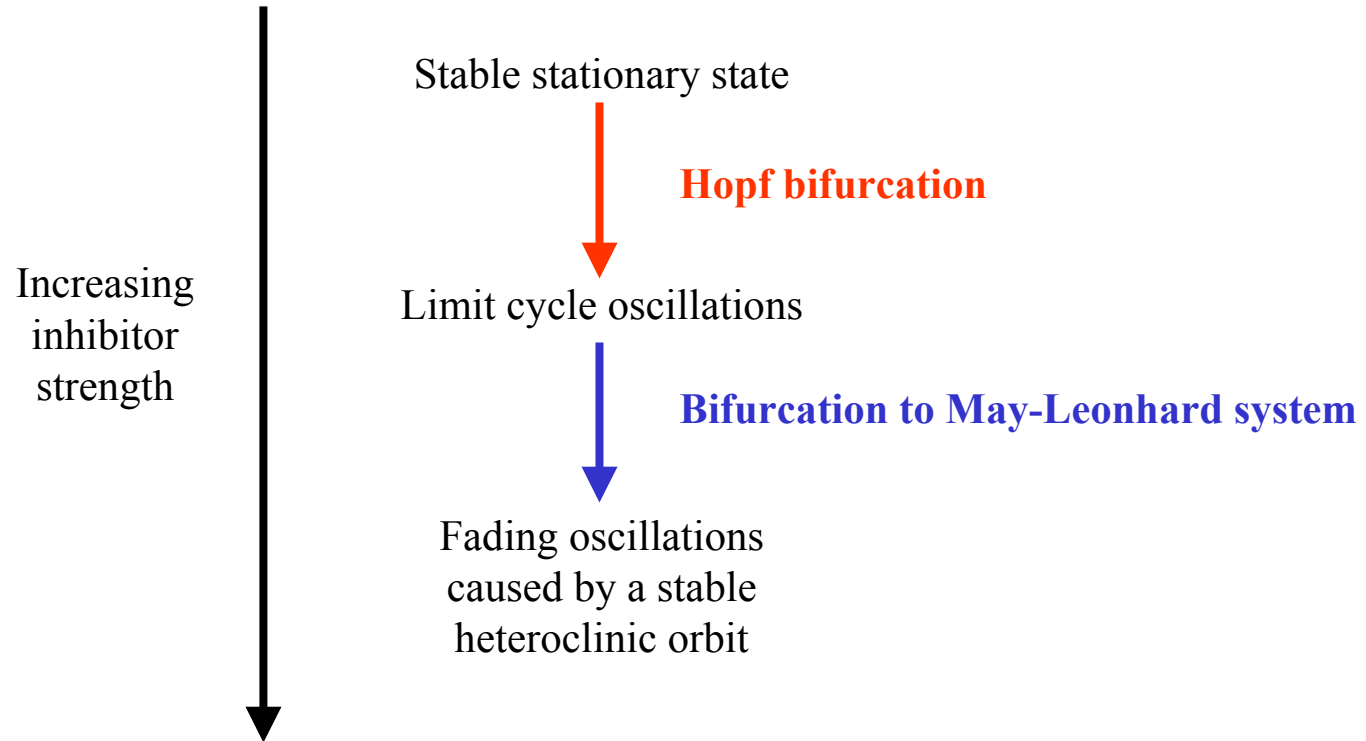
Regulatory dynamics at $D \leq 0$, rep.-rep., $n=2$

Hill coefficient: n	Act.-Act.	Act.-Rep.	Rep.-Rep.
1	S , E	S	S
2	E , B(E,P)	S	S , B(P_1, P_2)
3	E , B(E,P)	S , O	S , B(P_1, P_2)
4	E , B(E,P)	S , O	S , B(P_1, P_2)

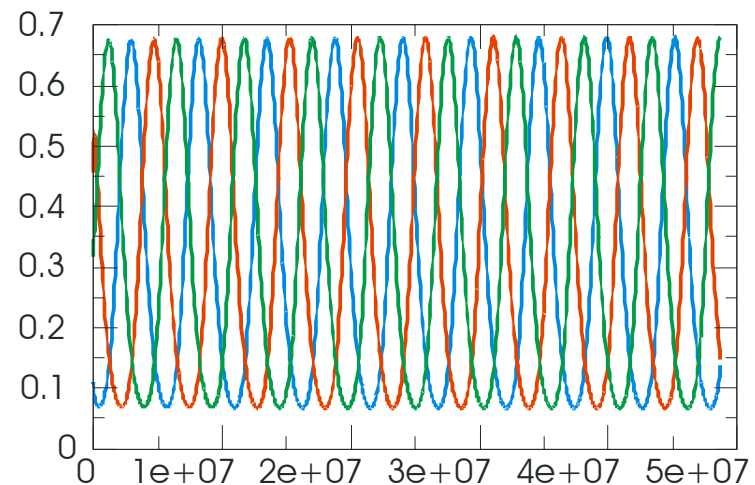


An example analyzed and simulated by MiniCellSim

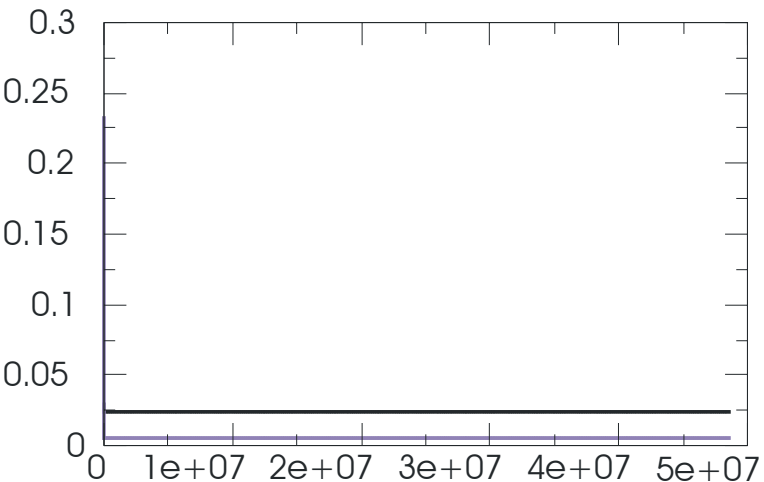
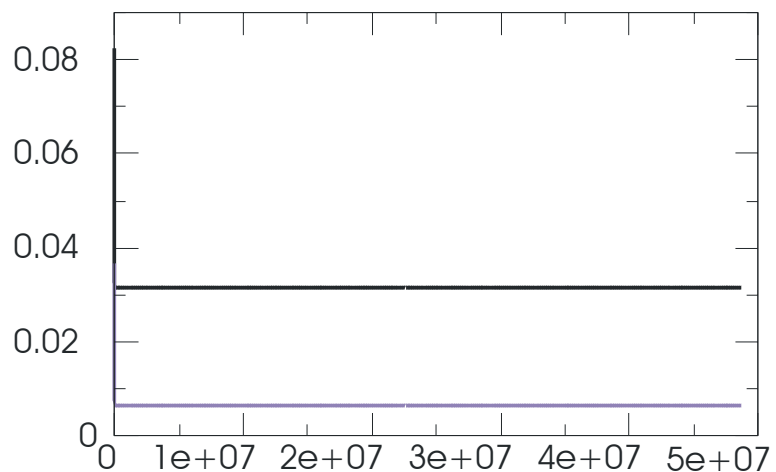
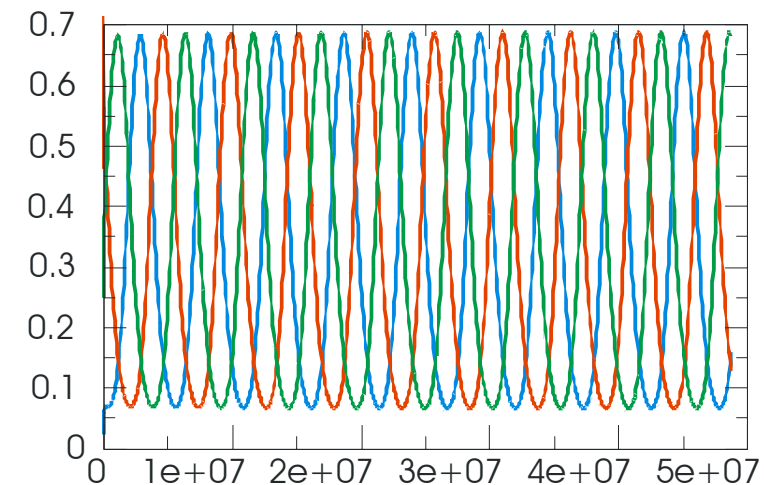
The repressilator: M.B. Elowitz, S. Leibler. A synthetic oscillatory network of transcriptional regulators. *Nature* **403**:335-338, 2002



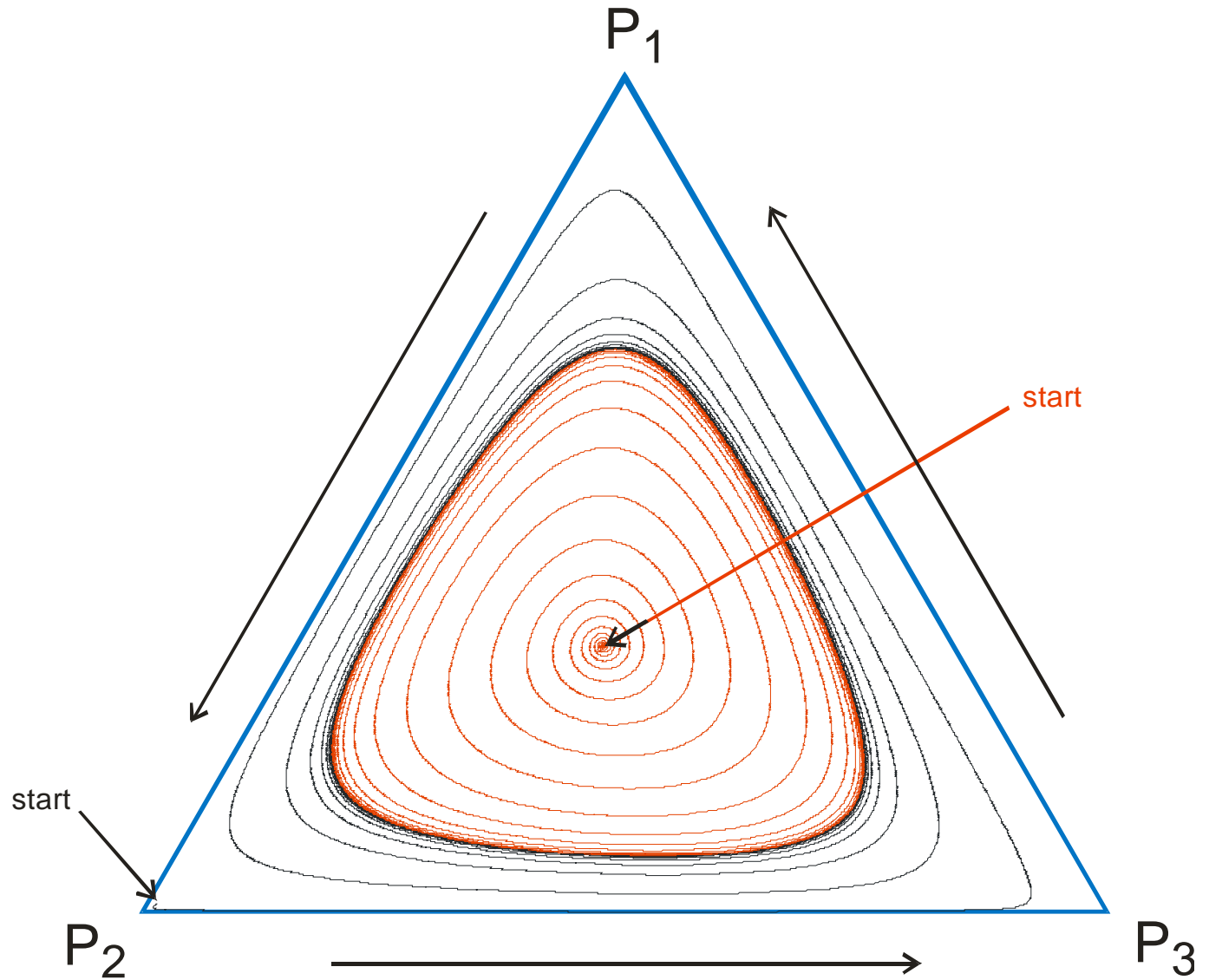
Proteins



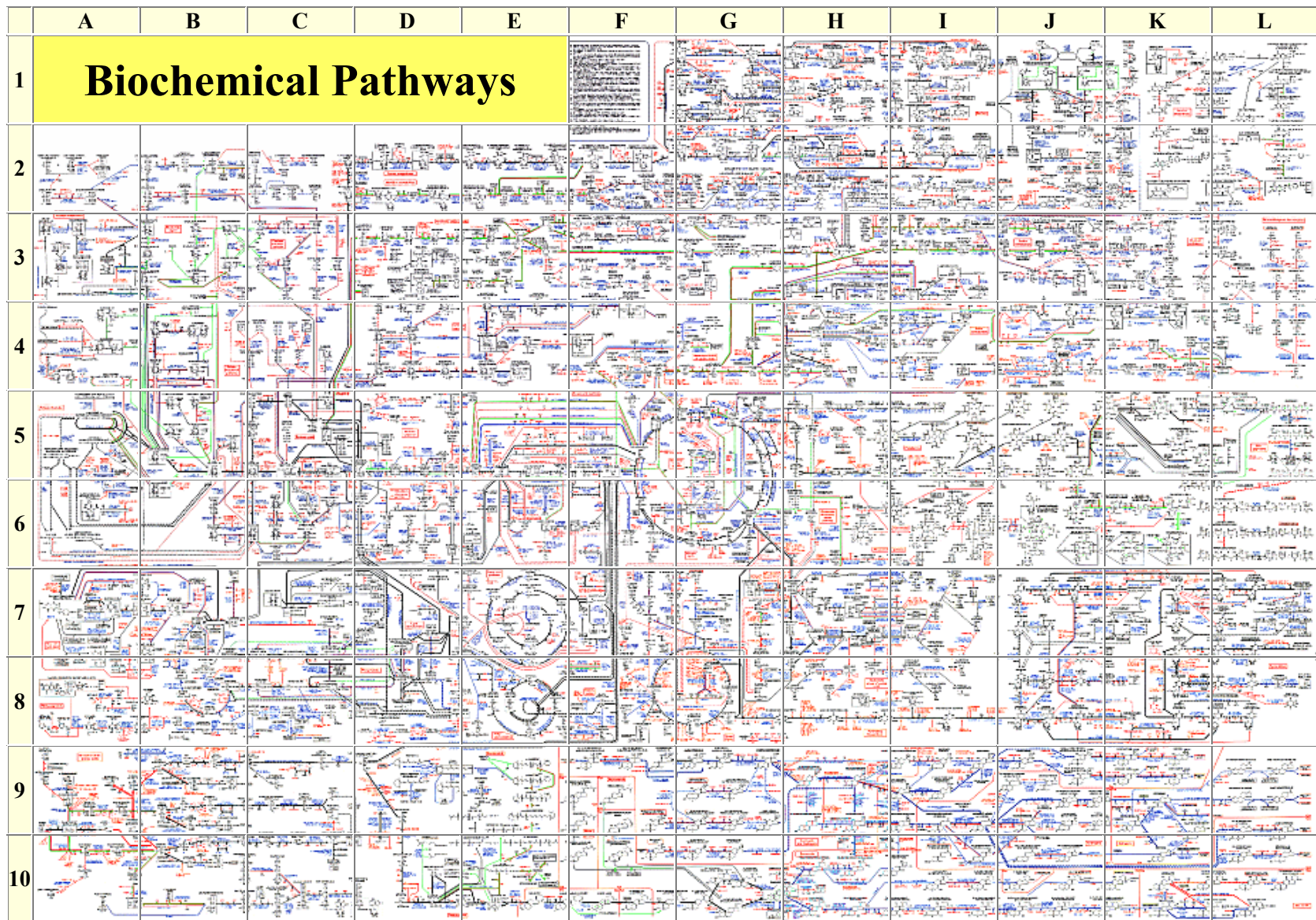
mRNAs



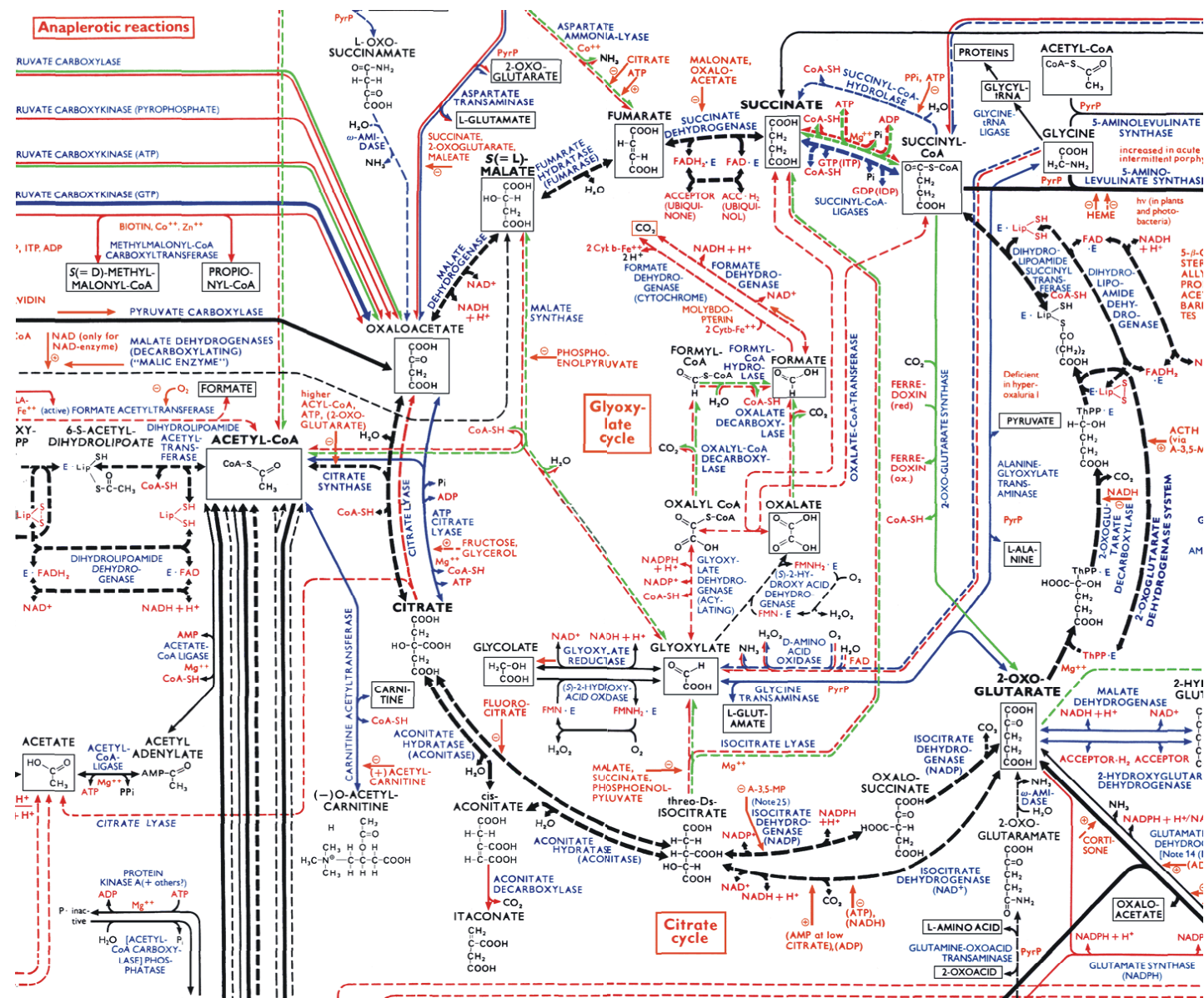
The repressilator limit cycle



The repressilator limit cycle

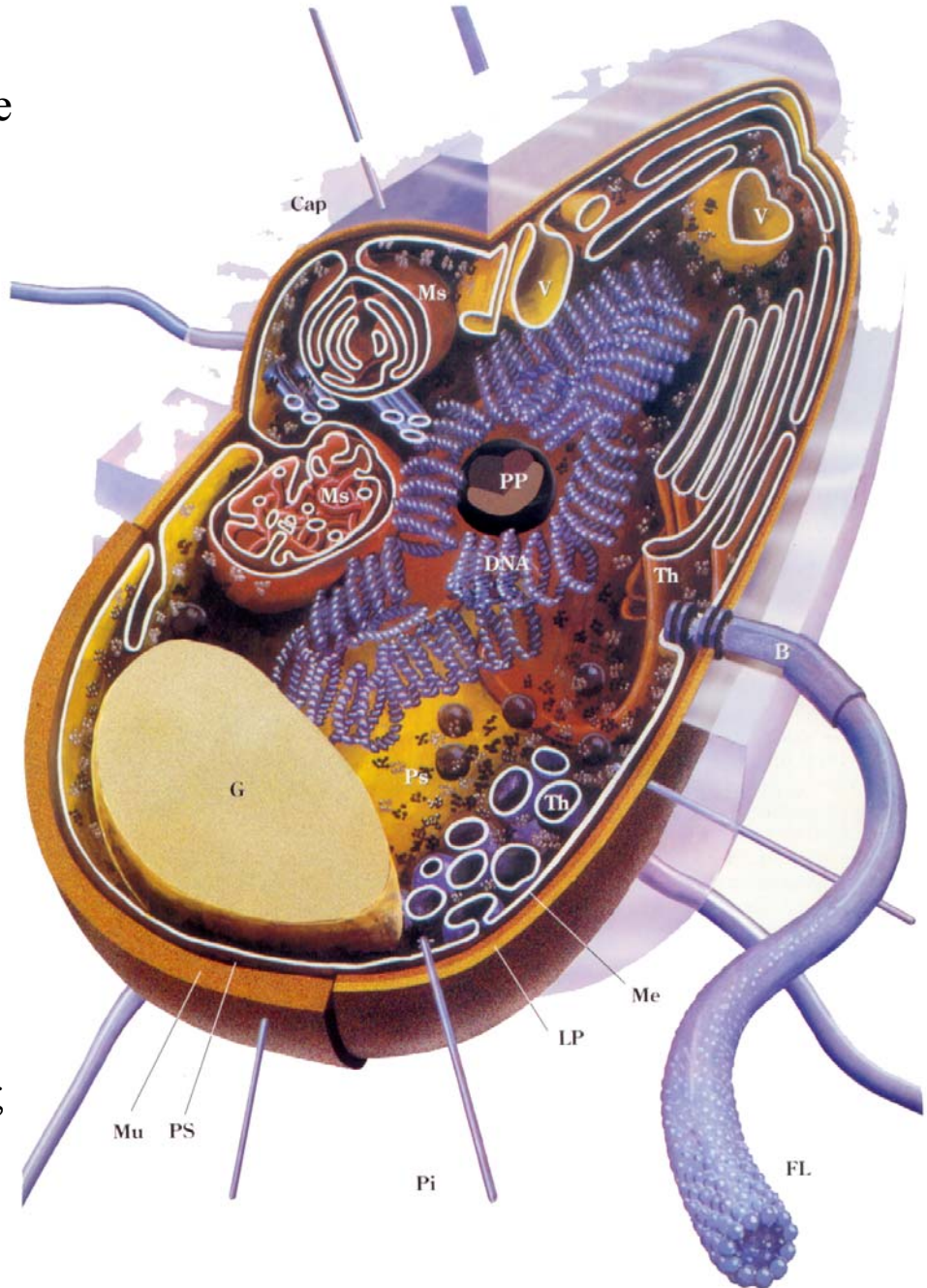


The reaction network of cellular metabolism published by Boehringer-Ingelheim.



The citric acid
or Krebs cycle
(enlarged from
previous slide).

The **bacterial cell** as an example for the simplest form of autonomous life

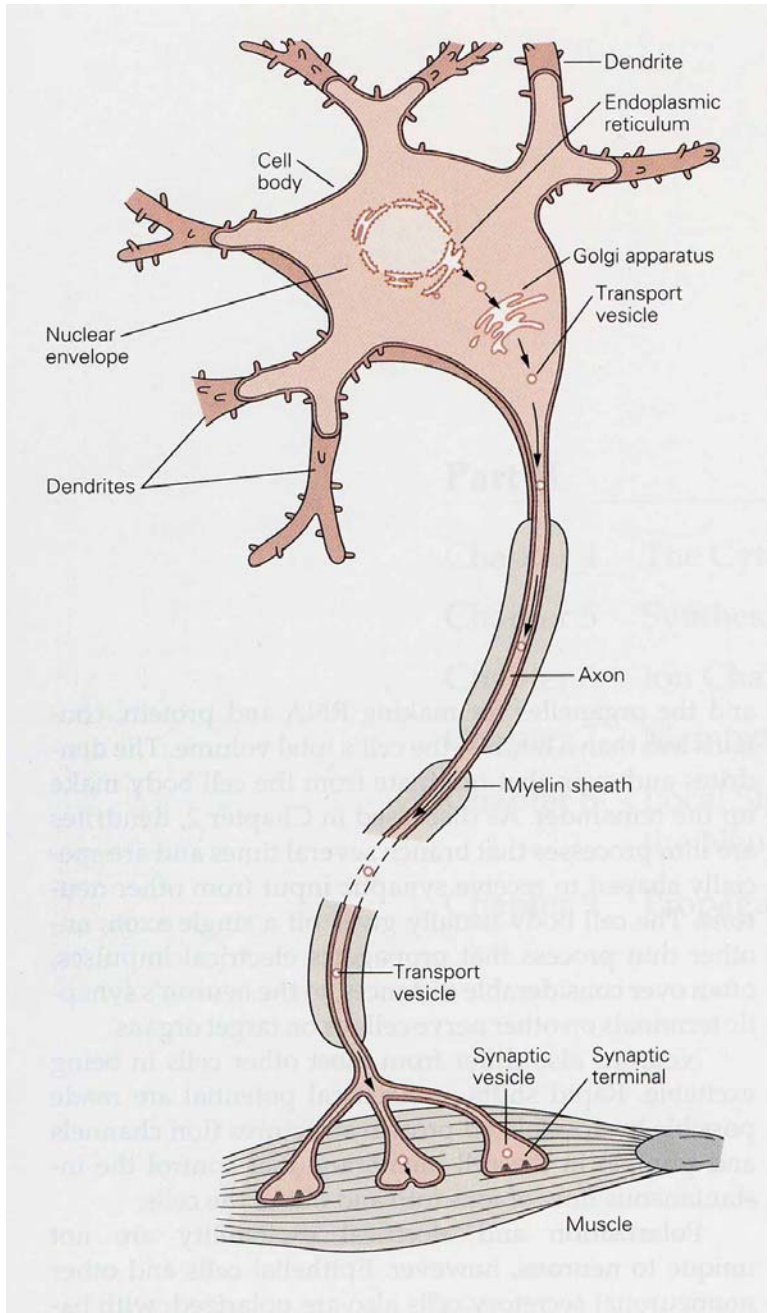


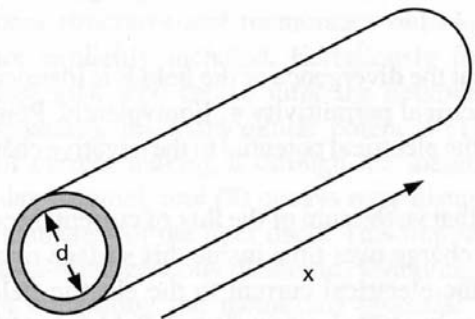
The **human body**:

10^{14} cells = 10^{13} eukaryotic cells +
≈ 9×10^{13} bacterial (prokaryotic) cells;
≈ 200 eukaryotic cell types

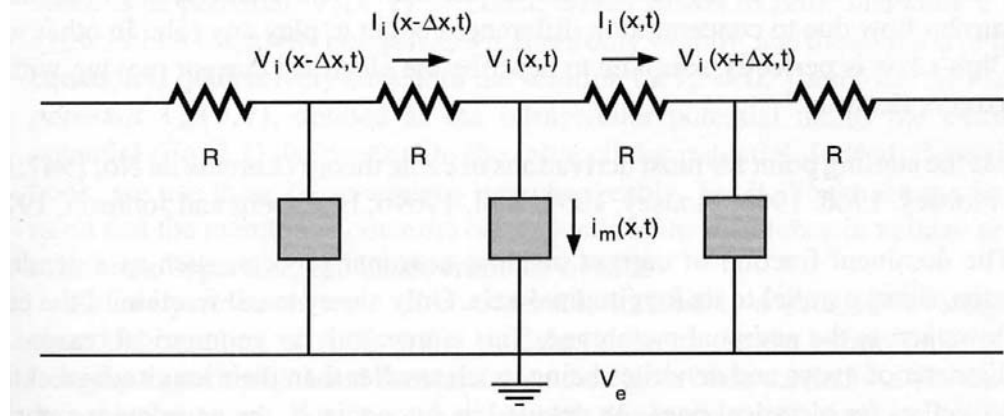
1. Equilibrium structures and dissipative patterns
2. Spatio-temporal patterns in chemical reactions
3. Patterns in development
4. Genetic and metabolic networks
- 5. Patterns in neurobiology**

A single neuron signaling to a muscle fiber





A



B

Fig. 2.2 ELECTRICAL STRUCTURE OF A CABLE (A) Idealized cylindrical axon or dendrite at the heart of one-dimensional cable theory. Almost all of the current inside the cylinder is longitudinal due to geometrical (the radius is much smaller than the length of the cable) and electrical factors (the membrane covering the axon or dendrite possesses a very high resistivity compared to the intracellular cytoplasm). As a consequence, the radial and angular components of the current can be neglected, and the problem of determining the potential in these structures can be reduced from three spatial dimensions to a single one. On the basis of the bidomain approximation, gradients in the extracellular potentials are neglected and the cable problem is expressed in terms of the transmembrane potential $V_m(x, t) = V_i(x, t) - V_e$. (B) Equivalent electrical structure of an arbitrary neuronal process. The intracellular cytoplasm is modeled by the purely ohmic resistance R . This tacitly assumes that movement of carriers is exclusively due to drift along the voltage gradient and not to diffusion. Here and in the following the extracellular resistance is assumed to be negligible and V_e is set to zero. The current per unit length across the membrane, whether it is passive or contains voltage-dependent elements, is described by i_m and the system is characterized by the second-order differential equation, Eq. 2.5.

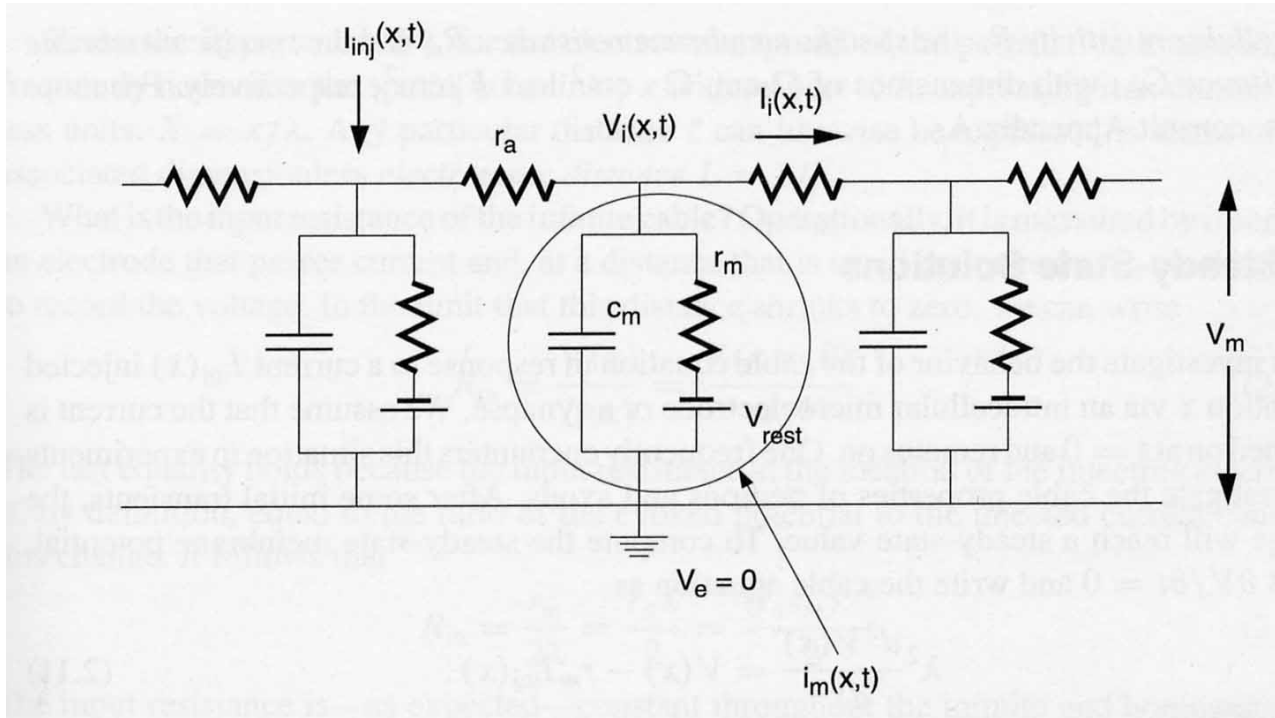


Fig. 2.3 A SINGLE PASSIVE CABLE Equivalent lumped electrical circuit of an elongated neuronal fiber with passive membrane. The intracellular cytoplasm is described by an ohmic resistance per unit length r_a and the membrane by a capacitance c_m in parallel with a passive membrane resistance r_m and a battery V_{rest} . The latter two components are frequently referred to as *leak resistance* and *leak battery*. An external current $I_{\text{inj}}(x, t)$ is injected into the cable. The associated linear cable equation (Eq. 2.7) describes the dynamics of the electrical potential $V_m = V_i - V_e$ along the cable.

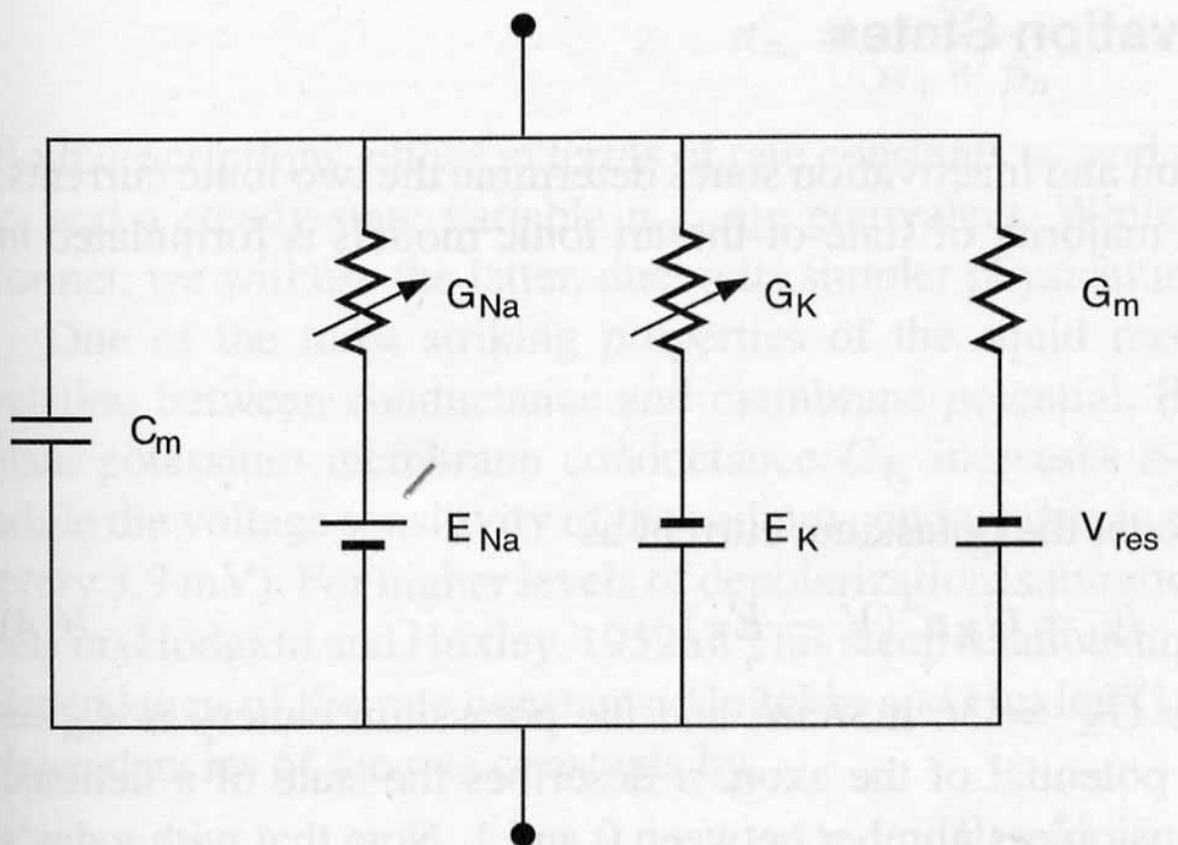


Fig. 6.2 ELECTRICAL CIRCUIT FOR A PATCH OF SQUID AXON
 Hodgkin and Huxley modeled the membrane of the squid axon using four parallel branches: two passive ones (membrane capacitance C_m and the leak conductance $G_m = 1/R_m$) and two time- and voltage-dependent ones representing the sodium and potassium conductances.

Hodgkin-Huxley OD equations

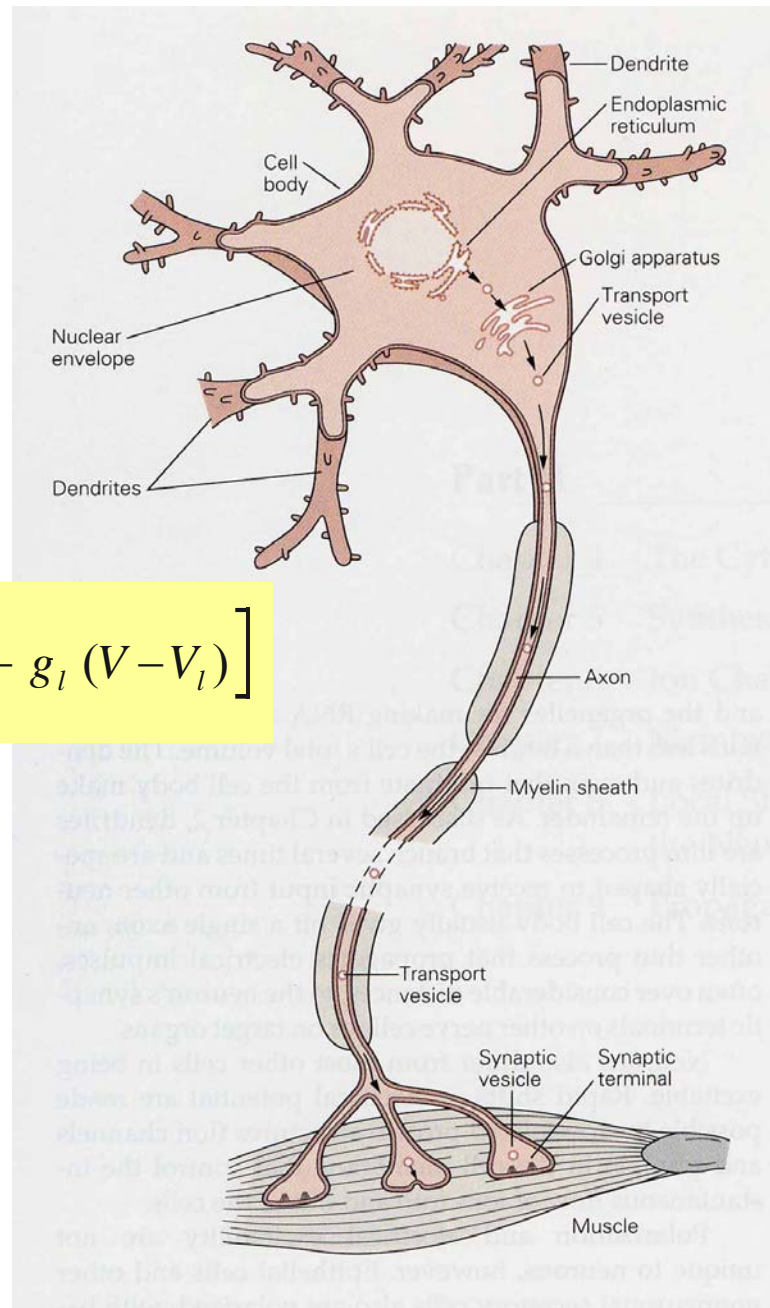
$$\frac{dV}{dt} = \frac{1}{C_M} \left[I - g_{Na} m^3 h (V - V_{Na}) - g_K n^4 (V - V_K) - g_l (V - V_l) \right]$$

$$\frac{dm}{dt} = \alpha_m (1-m) - \beta_m m$$

$$\frac{dh}{dt} = \alpha_h (1-h) - \beta_h h$$

$$\frac{dn}{dt} = \alpha_n (1-n) - \beta_n n$$

A single neuron signaling to a muscle fiber



$$\alpha_m = \frac{x}{e^x - 1}, \quad x = \frac{25 - V}{10} ; \quad \beta_m = 4 \exp \left[-\frac{V}{18} \right]$$

$$\alpha_h = 0.07 \exp \left[-\frac{V}{20} \right] ; \quad \beta_h = \frac{1}{e^x - 1}, \quad x = \frac{30 - V}{10}$$

$$\alpha_n = \frac{x}{10(e^x - 1)}, \quad x = \frac{10 - V}{10} ; \quad \beta_n = 0.125 \exp \left[-\frac{V}{80} \right]$$

Gating functions of the Hodgkin-Huxley equations

$$\frac{\partial m}{\partial t} = \Theta(T) [\alpha_m(1 - m) - \beta_m m]$$

$$\frac{\partial h}{\partial t} = \Theta(T) [\alpha_h(1 - h) - \beta_h h]$$

$$\frac{\partial n}{\partial t} = \Theta(T) [\alpha_n(1 - n) - \beta_n n] ,$$

where $\Theta(T) = 3^{(T-6.3)/10}$

Temperature dependence of the Hodgkin-Huxley equations

$$\frac{dV}{dt} = \frac{1}{C_M} \left[I - \bar{g}_{Na} m^3 h (V - V_{Na}) - \bar{g}_K n^4 (V - V_K) - \bar{g}_l (V - V_l) \right]$$

$$\frac{dm}{dt} = \alpha_m (1-m) - \beta_m m$$

$$\frac{dh}{dt} = \alpha_h (1-h) - \beta_h h$$

$$\frac{dn}{dt} = \alpha_n (1-n) - \beta_n n$$

Hodgkin-Huxley OD equations



Hhsim (2).lnk

Simulation of space independent Hodgkin-Huxley equations:
Voltage clamp and constant current

$$\frac{1}{R} \frac{\partial^2 V}{\partial x^2} = C \frac{\partial V}{\partial t} + \left[g_{Na} m^3 h (V - V_{Na}) + g_K n^4 (V - V_K) + g_l (V - V_l) \right] 2\pi r L$$

$$\frac{\partial m}{\partial t} = \alpha_m (1-m) - \beta_m m$$

$$\frac{\partial h}{\partial t} = \alpha_h (1-h) - \beta_h h$$

$$\frac{\partial n}{\partial t} = \alpha_n (1-n) - \beta_n n$$

Hodgkin-Huxley PDEquations

Travelling pulse solution: $V(x,t) = V(\xi)$ with
 $\xi = x + \theta t$

Hodgkin-Huxley equations describing pulse propagation along nerve fibers

$$\frac{1}{R} \frac{d^2 V}{d \xi^2} = C_M \theta \frac{d V}{d \xi} + \left[\bar{g}_{Na} m^3 h (V - V_{Na}) + \bar{g}_K n^4 (V - V_K) + \bar{g}_l (V - V_l) \right] 2\pi r L$$

$$\theta \frac{d m}{d \xi} = \alpha_m (1-m) - \beta_m m$$

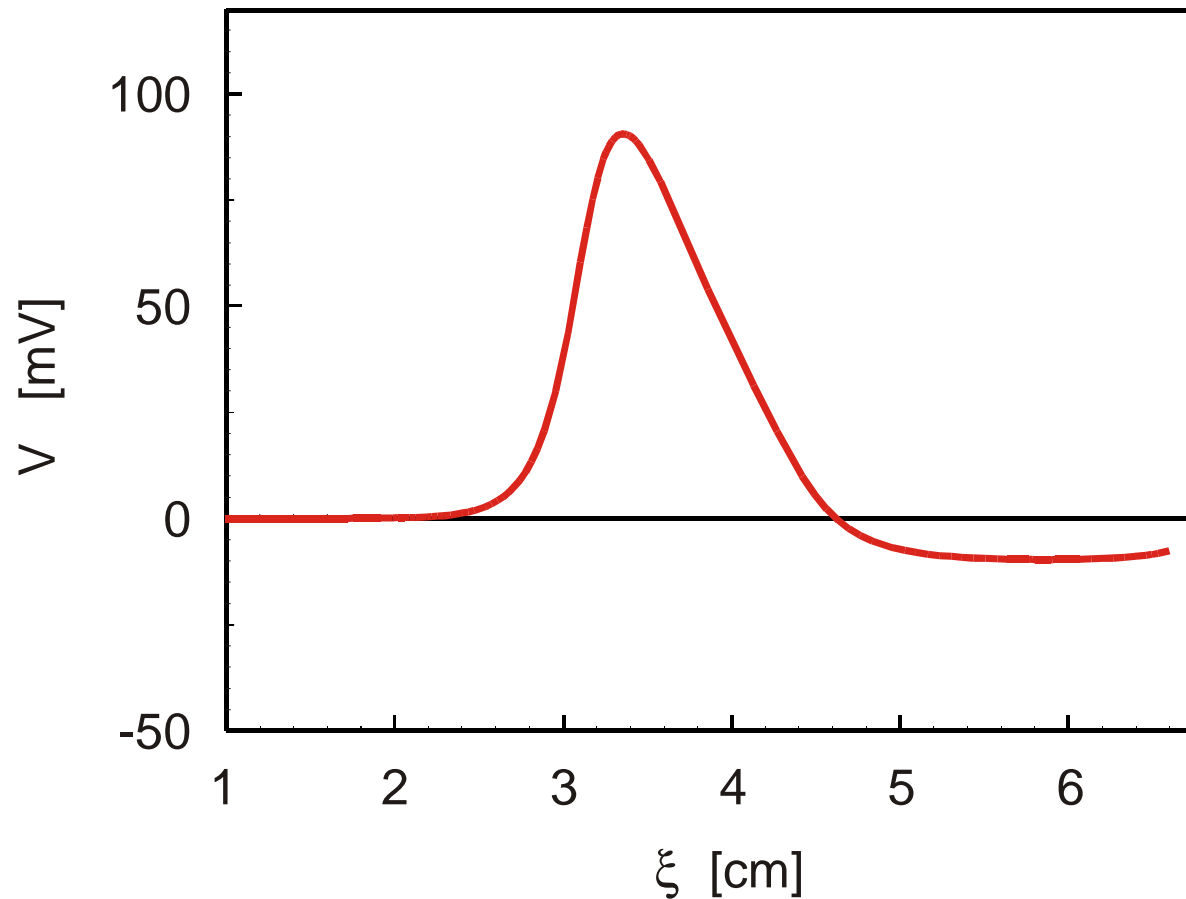
$$\theta \frac{d h}{d \xi} = \alpha_h (1-h) - \beta_h h$$

$$\theta \frac{d n}{d \xi} = \alpha_n (1-n) - \beta_n n$$

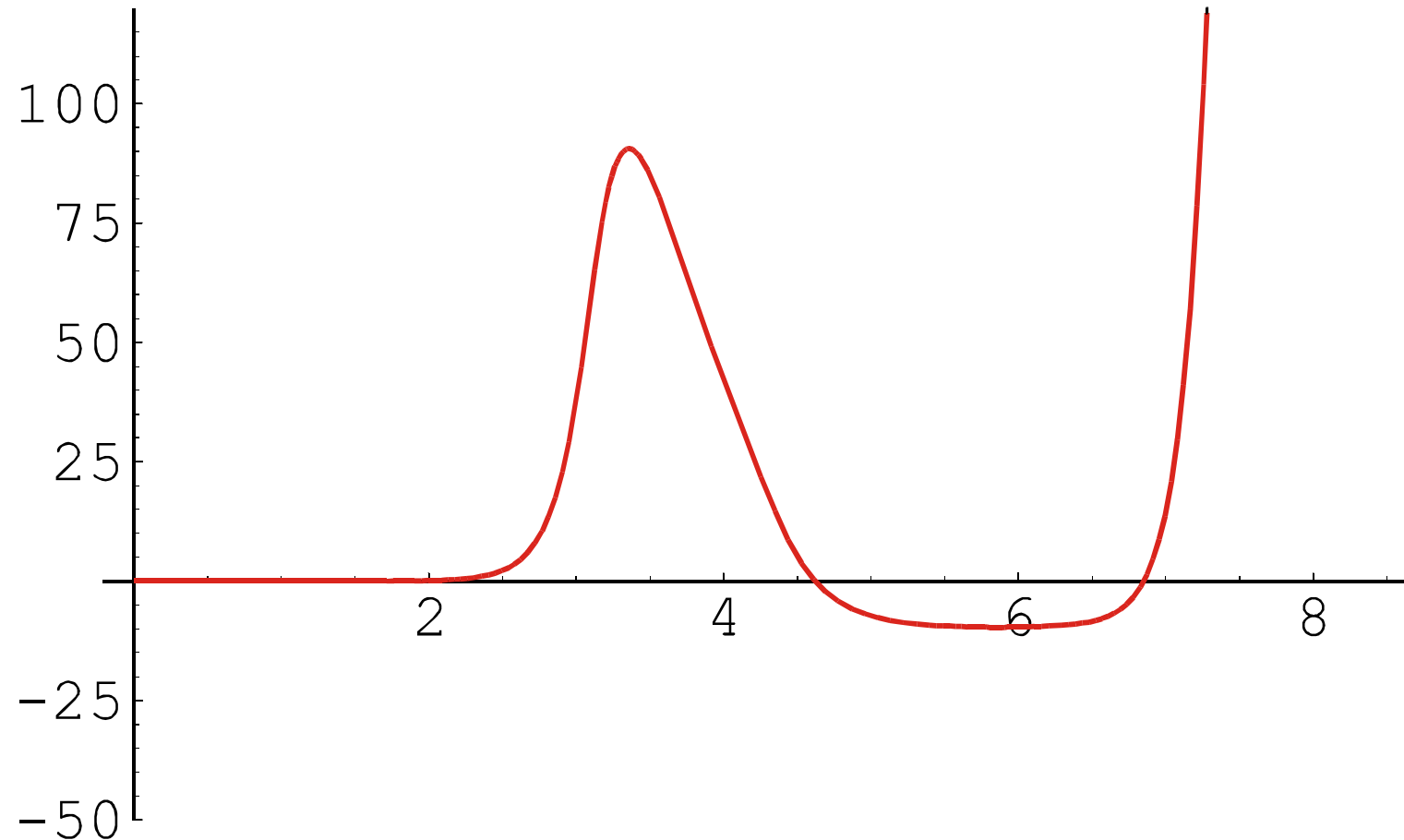
Hodgkin-Huxley PDEquations

Travelling pulse solution: $V(x,t) = V(\xi)$ with
 $\xi = x + \theta t$

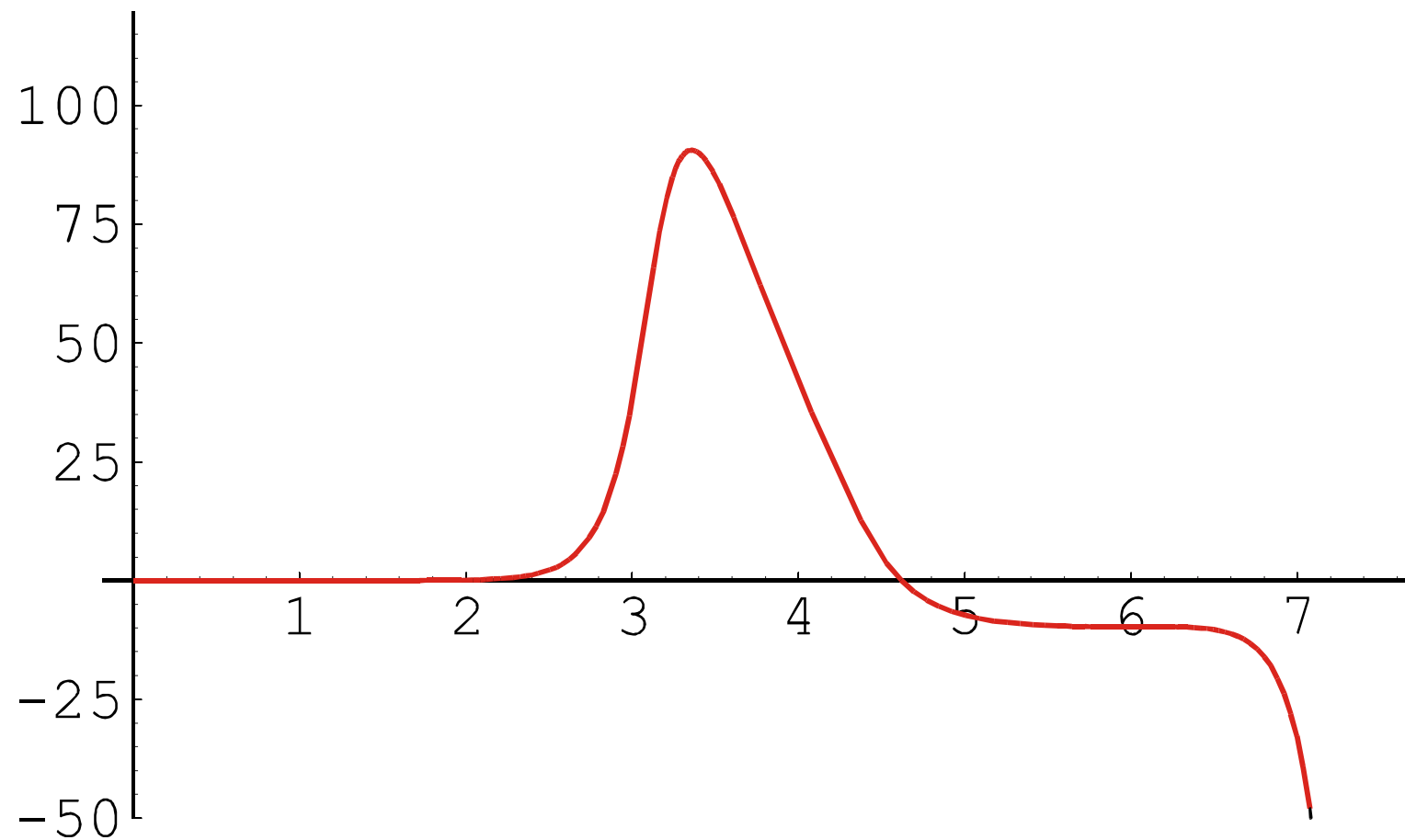
Hodgkin-Huxley equations describing pulse propagation along nerve fibers



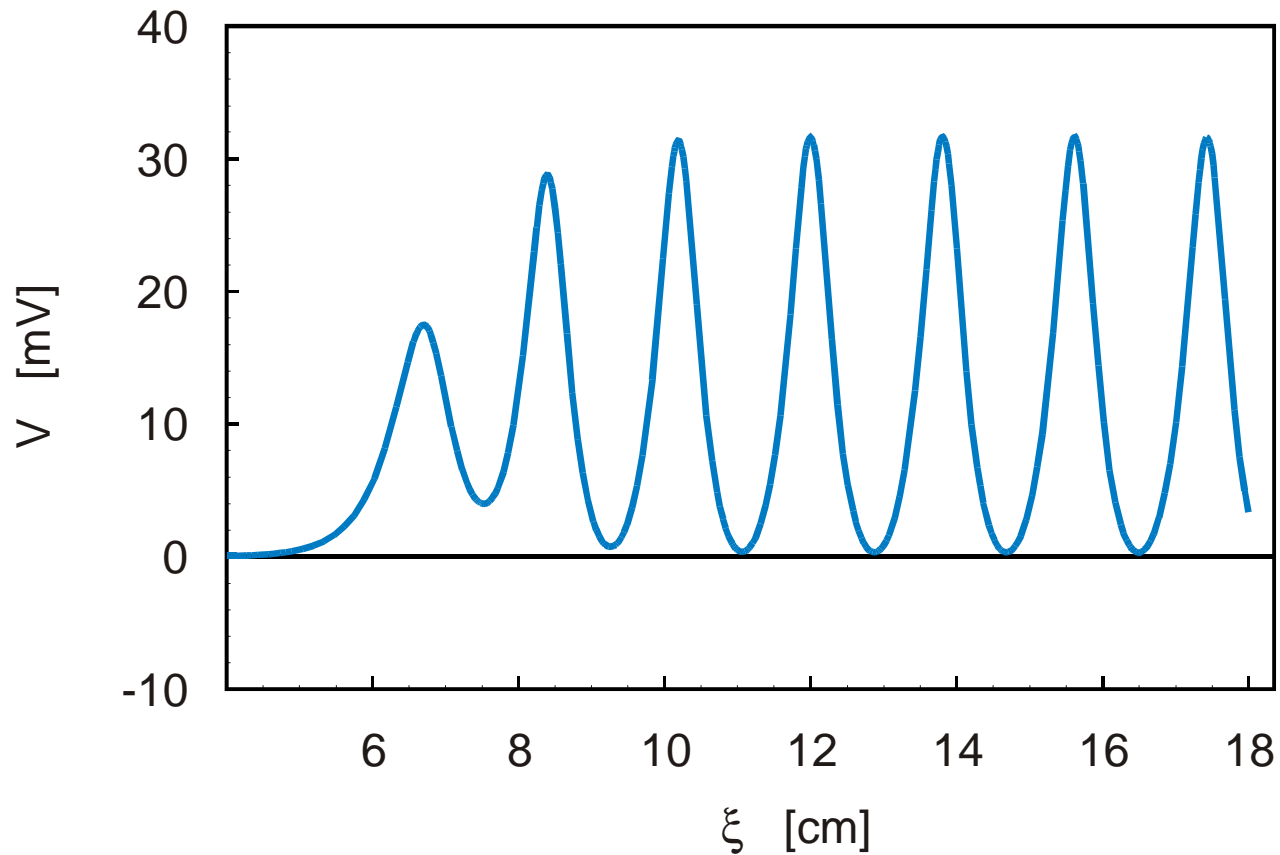
$T = 18.5 \text{ C}$; $\theta = 1873.33 \text{ cm / sec}$



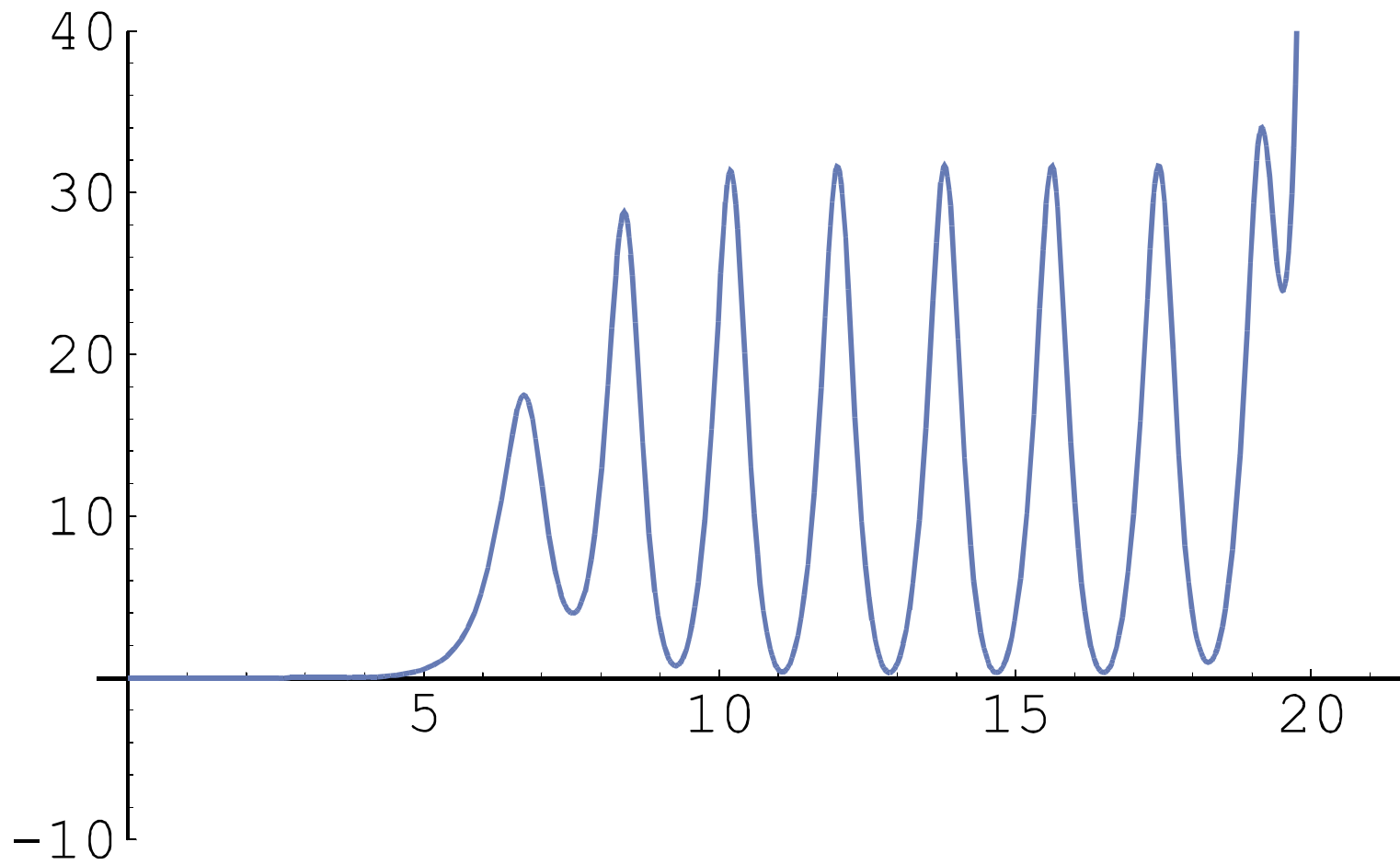
$T = 18.5 \text{ C}$; $\theta = 1873.3324514717698 \text{ cm / sec}$



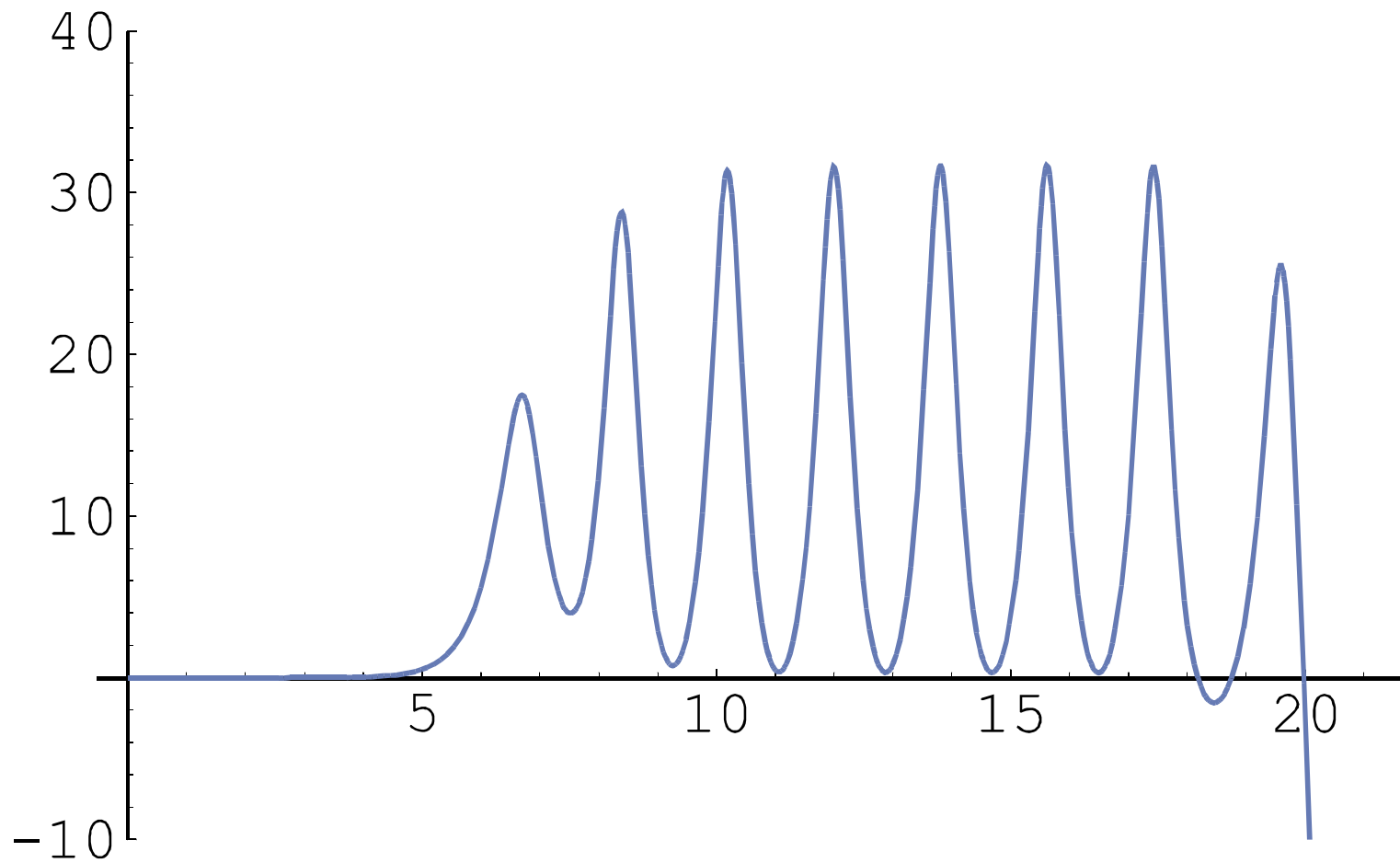
$T = 18.5 \text{ C}$; $\theta = 1873.3324514717697 \text{ cm / sec}$



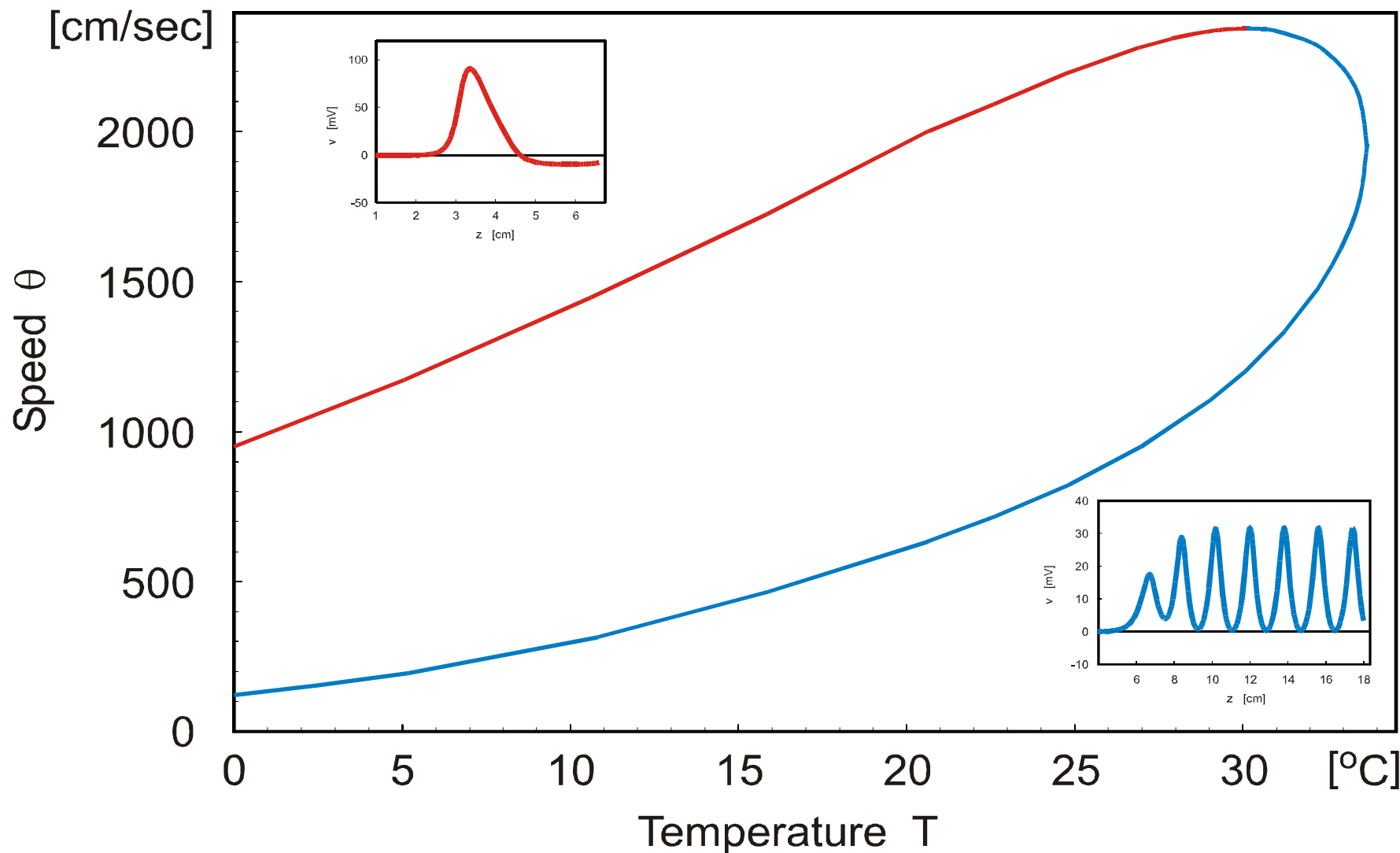
$T = 18.5$ C; $\theta = 544.070$ cm / sec



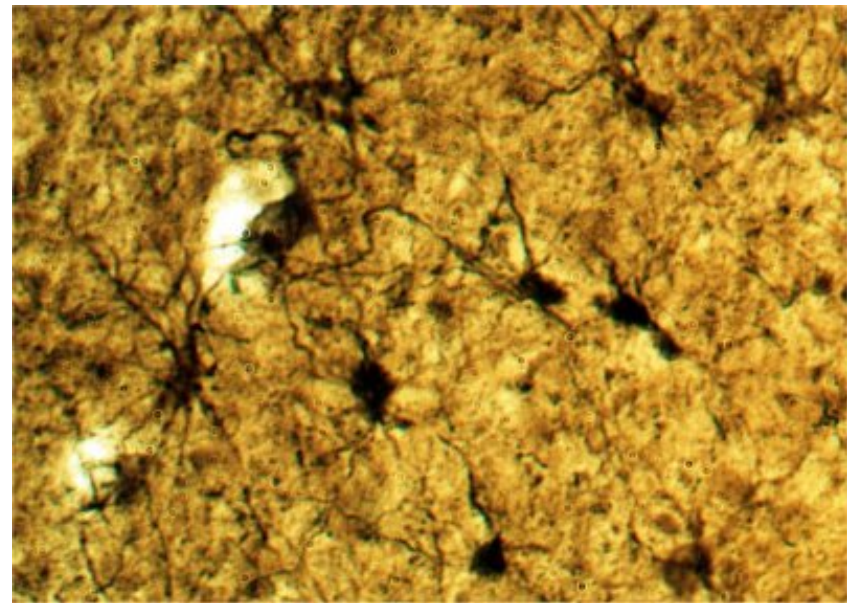
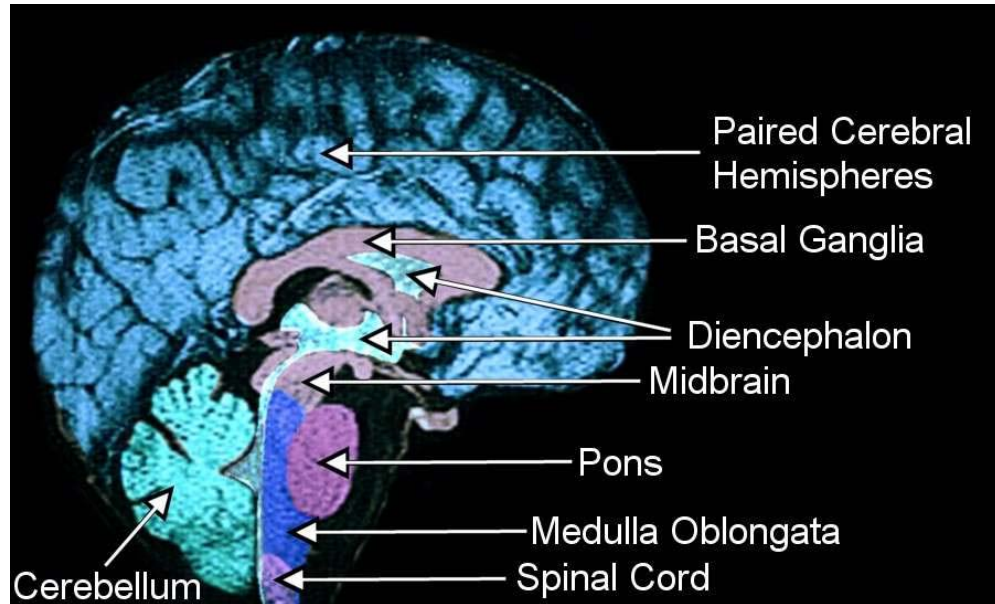
$T = 18.5 \text{ C}$; $\theta = 554.070286919319 \text{ cm/sec}$



$T = 18.5 \text{ C}; \theta = 554.070286919320 \text{ cm/sec}$



Propagating wave solutions of the Hodgkin-Huxley equations



The human brain

10^{11} neurons connected by $\approx 10^{13}$ to 10^{14} synapses



Acknowledgement of Support

Universität Wien

Fonds zur Förderung der wissenschaftlichen Forschung (FWF)
Projects No. 14898

Wiener Wissenschafts-, Forschungs- und Technologiefonds (WWTF)
Project No. Mat05

Österreichischen Akademie der Wissenschaften

Universität Wien and the Santa Fe Institute



Universität Wien

Contributors

Christoph Flamm, Gottfried Köhler, Andreas Svrček-Seiler, Stephanie Widder,
Universität Wien, AT

Erwin Gaubitzer, Lukas Endler and Rainer Machne, Universität Wien, AT

Heinz Engl, Philipp Kuegler, James Lu, Stephan Müller, RICAM Linz

Paul Phillipson, University of Colorado, Boulder

Web-Page for further information:

<http://www.tbi.univie.ac.at/~pks>

